NASA CR-54904
LAC ER-8372

EFFECT OF NUCLEAR RADIATION ON MATERIALS AT CRYOGENIC TEMPERATURES

by

LOCKHEED NUCLEAR PRODUCTS

C. A. Schwanbeck, Project Manager

prepared for

NATIONAL AERONAUTICS AND SPACE ADMINISTRATION

Contract NAS3—7985

NOTICE

Requests for copies of this report should be referred to

National Aeronautics and Space Administration
Office of Scientific and Technical Information
Attention: AFSS-A
Washington, D.C. 20546

NASA CR-54904
LAC ER-8372

QUARTERLY REPORT NO. 2

October 21, 1965 Through January 21, 1966

EFFECT OF NUCLEAR RADIATION ON MATERIALS AT CRYOGENIC TEMPERATURES

by

LOCKHEED NUCLEAR PRODUCTS

C. A. Schwanbeck, Project Manager

prepared for

NATIONAL AERONAUTICS AND SPACE ADMINISTRATION

February 1966

Contract NAS 3-7985

Technical Management
NASA Lewis Research Center
Cleveland, Ohio
Nuclear Systems Division
Charles L. Younger

LOCKHEED NUCLEAR PRODUCTS
LOCKHEED-GEORGIA COMPANY

A DIVISION OF LOCKHEED AIRCRAFT CORPORATION

If this document is supplied under the requirements of a United States Government contract, the following legend shall apply unless the letter U appears in the coding box:

This data is furnished under a United States Government contract and only those portions hereof which are marked (for example, by circling, underscoring or otherwise) and indicated as being subject to this legend shall not be released outside the Government (except to foreign governments, subject to these same limitations), nor be disclosed, used, or duplicated, for procurement or manufacturing purposes, except as otherwise authorized by contract, without the permission of Lockheed-Georgia Company, A Division of Lockheed Aircraft Corporation, Marietta, Georgia. This legend shall be marked on any reproduction hereon in whole or in part.

The "otherwise marking" and "indicated portions" as used above shall mean this statement and includes all details or manufacture contained herein respectively.

Code: U Contract: NAS 3-7985

FOREWORD

This quarterly report is submitted to the National Aeronautics and Space Administration, Lewis Research Center, by the Lockheed-Georgia Company in accordance with the requirements of NASA Contract NAS 3-7985.

TABLE OF CONTENTS

TABLE OF CONTENTS (Cont'd)

TABLE OF CONTENTS (Cont'd)

1 SUMMARY

This is the second Quarterly Progress Report on Contract NAS 3-7985, entitled, "The Effect of Nuclear Radiation on Materials at Cryogenic Temperatures." The scope of the test program as described in the first Quarterly Progress Report (NASA CR-54787, LAC ER-8231) has been amended to include irradiations of Aluminum 1099 to only 5×10^{15} and 5×10^{16} nvt (E>0.5 mev), and studies of the self annealing at various temperatures of irradiation effects observable by testing at 30°R.

Progress during this reporting period has consisted of: necessary preparation and some modifications of existing equipment, completed tensile test results from Titanium 55A and partial tensile test results from Aluminum 1099.

The refrigeration system and other test equipment have performed very well, resulting in unusually efficient use of available neutron flux during this reporting period.

The flux mapping required by a new beam port gamma shield is complete. There is no significant change in neutron flux level due to the shield change.

Temperature correlations and development of annealing temperature control methods are complete.

The test loop alignment problem, discussed in detail in the first quarterly report, does not appear as serious with the loop to be modified for fatigue testing as it was with the prototype loop. Strengthening of the structural member of this loop is not required.

Component parts of the new load control system have been delivered and will be installed early in the next reporting period.

Progress during the first quarter of Contract NAS 3-7985 was in the form of necessary preparations and modifications of existing test loops with no actual test results.

Progress during this reporting period (second quarter of Contract NAS 3-7985) has consisted of continued necessary preparations and modifications of existing equipment, completed tensile test results from Titanium 55A and partial tensile test results from Aluminum 1099. The pertinent information is reported in the following sections.

2 INTRODUCTION

The combination of a fast neutron and cryogenic environment encountered in the structural members of a liquid hydrogen nuclear rocket imposes service conditions dissimilar to those encountered in other engineering applications. Both fast neutron bombardment and extremely low temperatures affect the mechanical properties of engineering materials; therefore the magnitude of the combined effect must be determined to provide basic design information before materials for a reliable nuclear rocket system can be selected. Since the neutron irradiation effects will spontaneously anneal even at low temperatures, tests to provide the desired information concerning the combined effect must be conducted with the specimens held at the temperature of interest during the entire irradiation and testing period.

A screening program (ref. 1) was undertaken to assess the effect of fast neutron irradiation on selected engineering alloys at temperatures near the boiling point of liquid hydrogen (-423°F). Tensile tests on parallel sample sets of unnotched specimens for each alloy at room temperature unirradiated, at 30°R (-430°F) unirradiated and at 30°R irradiated to 1×10^{17} nvt (energies greater than 0.5 Mev) were performed at the NASA Plum Brook Reactor Facility using a helium refrigerator and testing equipment specially designed for in-pile testing under controlled temperature conditions.

Test results from the screening program indicated that titanium alloys possessed the highest strength-to-weight ratio following exposure to the combined nuclear-cryogenic environment as well as being among the least susceptible to deterioration of mechanical properties of the alloys tested. On the other hand, Aluminum 1099 (99.99% Aluminum) was found to be very sensitive to both irradiation and temperature of irradiation.

Based on the information obtained from the screening program, an in-pile test program (see section 5) has been initiated to study in greater detail the effects of a combined nuclear-cryogenic environment on the mechanical properties of metals. The objective of this program is to provide engineering data at higher flux levels and/or under different load conditions than heretofore attained at cryogenic temperatures as well as data for more fundamental studies. Its scope consists of two general phases, tensile testing and low-cycle fatigue testing. The tensile testing phase includes irradiations at 30°R to 10^{18} nvt (E>0.5 Mev),

---

(1). References appear in section 7.

irradiations to 10^{17} nvt ($E > 0.5$ Mev) at temperatures between 30°R and room temperature (540°R), and irradiations to 10^{17} nvt ($E > 0.5$ Mev) at 30°R followed by specimen warm-up prior to fracture. The low-cycle fatigue testing phase includes both fatigue testing during irradiation at 30°R and fatigue testing following irradiation at 30°R to 10^{17} nvt ($E > 0.5$ Mev).

Existing test equipment (see section 3) will be utilized during performance of the test program. Most of this equipment has recently undergone major overhaul and modification (ref. 2) in preparation for the nominal 140 hour test period to obtain 10^{18} nvt ($E > 0.5$ Mev) exposures. Maintenance and calibration schedules, established during this overhaul effort, should keep the equipment operating reliably.

The tensile testing phase of the test program will precede the fatigue testing phase due to extensive modification of test loops and the hydraulic load control system necessary for cyclic loading. A qualification procedure is being conducted to demonstrate the adequacy of the test equipment for the tensile testing phase of the program as well as to give some additional data points. This qualification is required because of the organic seals which are used in the test loops to isolate the static helium refrigerant, under pressure in the head assembly, from the cooling water. These seals have operated satisfactorily to 10^{17} nvt ($E > 0.5$ Mev) irradiations but there was not assurance that they will retain their sealing characteristics after irradiations to 10^{18} nvt. Tests to 3×10^{17} nvt and 6×10^{17} nvt at 30°R have been performed before undertaking the experiments which require 10^{18} nvt.

As in the screening program (ref. 1), standard test specimens cannot be used in this test program due to various restrictions on the test equipment imposed by the nuclear cryogenic environment. The tensile specimens to be used represent a miniaturization of the standard ASTM E-8 specimen (ref. 3). Although fatigue specimen design is not as standardized as tensile specimen design, the miniature fatigue specimens used in this program will represent a departure from any commonly used design, but are similar in geometry to those used by other investigators (ref. 4).

A newly designed and fabricated gamma shield has been installed in the Plum Brook Reactor HB-2 beam port irradiation facility. This change requires new calibrations (see section 4), including neutron flux mapping and temperature correlations.

3 TEST EQUIPMENT

3.1 IDENTIFICATION

The test equipment for in-pile and out-of-pile testing under controlled temperature and load conditions permits the test program to be performed wholly by remote operations. Major components of the test equipment and the test operation can be readily identified by reference to figure 1. This equipment and its operation, described previously (ref. 5), is separated into six categories, shown schematically in figure 2, with information pertinent to the design, modification, and performance characteristics discussed in the following sections. Test equipment maintenance and hazards analyses are discussed separately in sections 3.8 and 3.9, respectively.

3.2 TEST LOOPS

The test loops are stainless steel cylindrical envelopes, six inches OD by about nine feet long, containing all necessary equipment for irradiating a test specimen at controlled temperature conditions and fracturing the specimen, at temperature, in tension or compression without removal from the irradiation field. At the aft end of the test loops, fittings are provided to connect the refrigeration system, the load control system, and the instrumentation and data recording system. Other fittings are provided for test loop cooling using deionized water (which must be isolated from the helium refrigerant).

To perform the test program, five tension-compression test loops are currently being used as follows:

Test loops 201-001 (the prototype loop) and 201-005 -- design studies to determine modification requirements for low-cycle fatigue testing. (see section 3.2.2)

Test loop 201-002 -- in hot laboratory area where investigation of various methods of repairing the inner helium line are currently being evaluated (see section 3.8.2.1)

Test loops 201-003 and 201-004 -- used during reporting period for performing tensile test program (see section 3.2.1)

3.2.1 Tensile Test Loops

A test loop modification for elimination of a nuclear instrumentation seal, previously reported (ref. 5), is reclassified as maintenance and is discussed in section 3.8.2.1.4.

During this reporting period, test loop numbers 201-003 and 201-004 were used for a total of twenty-eight cycles* in performing temperature correlation, material evaluation, beam port flow evaluation and flux mapping studies.

Test loop 201-003 (with head assembly 201-011) was used for sixteen cycles of operation. However, during the ninth cycle of operation the load transducer signal was lost and repairs were required (see section 3.8.2.1).

Test loop 201-004 (with head assembly 201-006) was used for twelve cycles of operation. However, after completion of seven operational cycles an erratic signal from the LVDT load transducer required inspection and repair efforts (see section 3.8

The requirements for specimen change in the test loop are met with a removable test loop head. This requires the use of seals to isolate the static helium refrigerant, under pressure in the head assembly, from the cooling water. Organic seals used for this application performed satisfactorily after test specimen exposures to accumulated fluxes of 3×10^{17}, 6×10^{17}, and 1×10^{18} nvt (E>0.5 Mev). A few gas leaks were encountered upon removal of a test loop from the reactor beam port; however, these occurred at lower irradiation levels and appear to be a random event rather than a result of radiation damage. The organic seals are therefore considered qualified for use in performing the 10^{18}nvt (E>0.5 Mev) irradiations of the test program.

Very little can be said regarding the behavior of these seals as a function of irradiation in this application. The seals are made of polyurethane which, of all common organic seal materials, is known to be the most resistant to ionizing radiation. Radiation effects are attributed primarily to gamma exposure and depend on factors such as compression during irradiation, irradiation temperature and fabrication history.

---

* For cycle definition, see section 3.8.1.

Some density measurements have been made on the test loop seals after gamma doses of 2.5 x 10^8 r (during specimen exposure to 10^{17} nvt). Although the data showed large scatter, there appeared to be a measurable increase in the density corresponding to an increase in compression set. Such an increase in compression set would tend to cause leaks in this application, particularly if it is accompanied by a tendency to brittleness. The seals that were inspected, after identical irradiations, showed a large variation in physical properties (some being brittle while others were gummy) although they were identical materials, according to the manufacturer. Because of apparent unknown variations in the manufacturing process, further measurements are impractical and future efforts will be confined to qualitative observation of seals which fail during testing.

3.2.2 Fatigue Test Loops

Low-cycle axial tension-compression fatigue tests are to be performed using existing tension-compression test loops. The original specifications to which the test loops were constructed required that they be capable of exerting tensile or compressive loads, but not both in a cyclic manner. Specimen design and alignment features, incorporated in the specimen holders, which differed appreciably from those already used in the tensile tests were planned for the compressive tests. Considerable analysis and some modification is required before reliable tensile-compressive fatigue data can be obtained and the existing self-aligning features, suitable only for tensile loading, must be replaced by a more complex arrangement.

3.2.2.1 Design

An experimental determination of the alignment of load application, both in tension and compression, was initiated using the prototype tensile test loop (201-001) without the self-aligning features. During this reporting period, the preliminary fatigue (tension and compression) testing was changed to test loop 201-005. The major components of the test loop under consideration are shown in figure 3.

3.2.2.1.1 Structural Member

The structural member installed in the test loop, as shown in figure 3, is the assembly which supports the specimen loading actuator and also acts as a column directing the loads, which occur during loop insertion into the reactor beam port, into the carriage trunnion. The load applied in the test specimen is transmitted through the head assembly back through this member to the actuator. The load resulting from testing is distributed peripherally and transmitted eccentrically into the member.

As reported previously (ref. 5), a peripheral displacement occurred in the structural member of test loop 201-001 when loads were applied, and methods for modifying test loops to reduce this peripheral displacement were developed.

During this reporting period, and preliminary to modifying the structural member based on the deflections observed (and corrected to some extent in the prototype loop), deflection measurements were made on test loop 201-005. It was found that the deflections, under various tensile and compressive static loads, up to a maximum of 3550 pounds, were less than the deflections observed in the prototype loop. After careful checking, it was concluded that, due to increased stiffness of the structural assembly and probable improved alignment during construction, test loop 201-005 does not require modification of the structural member.

Additional support for this conclusion was obtained from strain gage measurements using an especially fabricated 5/16 inch specimen. These measurements gave a maximum differential strain between tensile fibers and compressive fibers in bending corresponding to a differential fiber stress of 7000 psi, which is well within allowable limits.

3.2.2.1.2 Pull Rod Linkage

The lost motion in the pull rod linkage of test loop 201-005 was assumed to be not significantly greater than the 0.02" measured in the prototype loop at 3500 pounds load (ref. 5). This assumption was based on the fact that the linkages are mechanically identical and was confirmed by loading responses on going from tension to compression, similar to those with the prototype loop.

3.2.2.1.3 Hydraulic Actuator Seals

As discussed in reference 5, the hydraulic actuator seals are being qualified for cyclic operation to 10,000 cycles. During that reporting period, over 1400 cycles at high loads with new seals, were obtained with test loop 201-001 without indication of failure. No significant additional testing of the seals in either test loop 201-001 or test loop 201-005 was performed during this reporting period.

3.2.2.1.4 Specimen Holders

The existing specimen holders are designed for self-alignment under tensile loading, using mating spherical seats. This feature cannot be used in axial tension-compression fatigue testing and therefore new specimen holders are required.

During this reporting period, the design of specimen holders for fatigue testing was completed. This design, shown in figure 4, is based on the performance of prototype holders and jam nuts with matching conical faces for maximum specimen alignment and minimum slack due to variations in thread dimensions. The system was designed using the smallest number of parts possible to minimize lost motion. This design also meets heat transfer requirements in that heat flow through the specimen is minimized.

3.2.2.1.5 Head Assembly Organic Seals For Fatigue Testing

The test loop head assembly organic seals for fatigue testing will be the same as those discussed in section 3.2.1 for tensile testing and will be subjected to more severe dynamic load conditions. Some difficulties are anticipated, particularly with irradiation. No difficulties have been experienced so far during the preliminary cyclic loading discussed in reference 5. However, to date, there has been no cyclic loading at low temperatures or in-pile.

3.2.2.2 Modification

After completion of the fatigue test loop modification requirements and detail design (section 3.2.2.1), it is planned to modify tensile test loop 201-005. During this modification, procedures will be developed for similar modification of one of the radioactive tensile test loops.

3.3 REFRIGERATION SYSTEM

The test specimen temperature is maintained at temperatures between 30°-540° Rankine using a gaseous phase helium refrigerator system. This system contains an electrically driven positive displacement compressor, counterflow heat exchanger and four reciprocating expansion engines. The system was specifically designed and fabricated for this application to provide a minimum of 1150 watts of refrigeration at 30°R. The system is capable of providing refrigeration for maintaining the specimen temperature at any temperature from 30°R to 540°R by varying engine speed, expansion engine pressure ratio, and the application of heat in manually controlled electrical resistance heaters installed in the refrigerant distribution manifold.

During this reporting period the system was operated satisfactorily for 1603.9 hours . Some difficulty was encountered in operation of the system to provide the limited refrigeration required to dissipate gamma heat at or near room temperature. The engines which were operating at low speed ultimately stalled when helium contaminants collected and froze in the cylinders. The system did provide the required refrigeration for a period exceeding six hours.

It is apparent that the operation of the system with the high pressure side of the heat exchanger at or near room temperature and the significant reduction of the temperature through the engines will cause deposition of any contaminants, such as water, in the engines.

The elimination of all the moisture in the helium supply is difficult inasmuch as any helium make-up in the expansion tank will tend to cumulatively add to the moisture in the system. In addition, the small quantities of moisture introduced when specimen change-over is performed will add to that already in the system. During low temperature operation this moisture will freeze out on the high pressure side heat exchanger surface and remain there to be removed by blow down when the refrigerator is warmed up.

Various methods of excluding the migration and freeze-out of helium contaminants in the system are currently being explored.

3.4 LOAD CONTROL SYSTEM

The existing specimen loading system for tensile testing utilizes a positive displacement pump with demineralized water as the working fluid to provide the pressure required by the hydraulic actuator positioned in the test loop. Strain rate can be controlled through a variable speed drive connected to the pump.

The load transducer is located in the test loop and the extensometer is positioned directly on the specimen to measure only the strain which occurs between the gage marks.

The pump and recording instrumentation are located in appropriate cabinets positioned on the grating above the quadrant at the 0'-0" level.

To perform the low-cyclic fatigue studies this system will be revised to provide a closed loop servo system as shown in figures 5 and 6. This system is described in more detail in reference 5.

The revised system includes an oil operated actuator mechanically coupled to another actuator using demineralized water as the working fluid. The latter provides the required flow and pressure to the actuator installed in the test loop.

The arrangement showing the servo controlled oil actuator and water operated actuator with associated valves and piping is shown in figure 7.

Installation design drawings for the system are nearly complete and will be submitted for approval during the next reporting period.

In addition, major components of the system have been received and system modification will proceed subsequent to drawing approval.

3.5 TRANSFER SYSTEM

To permit insertion and withdrawal of the test loops into the reactor pile, during reactor operation, a transfer system was designed and installed in quadrant D of the Plum Brook Reactor Facility. In addition, provision to change test specimens was incorporated by the installation of a hot cave with an access port in line with the assigned reactor beam port HB-2, as shown in figure 1.

To position the test loop for insertion or withdrawal from either the beam port or hot cave the supporting tables which are submerged approximately 20 feet in quadrant water, are aligned remotely using hydraulic pressure provided from an axial piston pump using demineralized water as a working fluid. After positioning, the loop carriage is coupled to the access port and the loop is inserted or withdrawn by a worm-drive screw arrangement driven by a hydraulic motor.

When the test loop is inserted into the beam port, it must overcome the reactor primary coolant water pressure of approximately 150 psig.

During the performance of a previous test program, a limitation on the fluid pressure to the hydraulic motor of 550 psig was imposed.

During this reporting period, the transfer system was used for a total of twenty-eight cycles* of test loop insertion and removal. The system performed satisfactorily during this operational time.

Also during this period the beam port gamma shield cooling water throttling location was changed from the outlet side of the shield, approximately 150 psig, to the inlet side, approximately 135 psig. This reduction in pressure materially reduces the thrust load on the test loop in driving a loop into the beam port and therefore allows the test loop drive system pressure to remain at approximately 550 psig while still maintaining a reasonable maintenance period on the test loop drive carriages.

3.6 SPECIMEN CHANGE EQUIPMENT

Due to the high activity level of the test loops after several in-pile exposures, remote handling techniques are required for changing specimens. The hot cave

---

* For cycle definition, see section 3.8.1.

that was installed was provided with manipulators, support fixtures and special tools to permit change-over of the specimen. In addition, minor repairs on the forward end of the test loop have been performed in this hot cave.

During this reporting period, the specimen change equipment was used for installation and removal of seventeen test specimens and seven foil packages. No specimen change equipment difficulties were encountered.

3.7 MISCELLANEOUS TEST EQUIPMENT

During this reporting period, two test loops were transferred to the hot laboratory work area for repair. After completing repair the loops were returned to the reactor containment vessel and positioned in quadrant D for use in the test program. The test loop transfers, using the test loop transfer cask and associated equipment, were performed in accordance with procedures previously described in reference 5.

3.8 TEST EQUIPMENT MAINTENANCE AND CALIBRATION

During this report period, the maintenance and calibration program previously developed by a reliability analysis was used to provide a scheduled equipment maintenance program. Forms for recording the operational history of the equipment were used together with maintenance logs to record the use and maintenance performed during test operations.

The proposed maintenance schedules were adhered to, inasmuch as possible, to perform routine inspection and repair. The repairs associated with any component or system malfunction were performed, time permitting, and the cause and nature of repair recorded in the maintenance log. Other repair activities which could not be completed during this reporting period are continuing as studies to provide definitive methods or techniques to effect repair, and will require substantial effort to complete.

3.8.1 Maintenance and Calibration Schedule

The projected maintenance schedules for the test equipment and refrigerator system are shown in figures 8 and 9. The schedules define the major sub-systems associated with the test equipment and the components contained therein that require periodic scheduled inspection, adjustment, repair and overhaul. To provide a common criteria for maintaining records of the use and performance of scheduled maintenance on the equipment, a use cycle was conceived and all the operational forms were altered to permit conformance with this cycle.

The cycle is as follows:

- Insertion into hot cave for specimen installation.
- Removal from hot cave after specimen installation.
- Insertion into reactor beam port for test irradiation.
- Withdrawal from beam port after completing test, and positioning the loop for insertion into the hot cave for specimen change-over.

Normal operation of all the test equipment listed in figure 8 will follow this cycle. In addition, this equipment will operate submerged in the quadrant water, and with the exception of the carriages and test loops, it is accessible for maintenance only when the quadrant is drained.

Deviation from the projected schedules are anticipated because scheduled maintenance will only be performed coincident with quadrant draining.

The projected refrigerator maintenance schedule (figure 9) is related to the hours of operation which are recorded cumulatively on a time meter which operates when the expansion engines are operating. The maintenance performed is recorded in a refrigerator maintenance log. Total operating time is also maintained by recording start-up and shut-down time on the refrigerator operation forms.

The transfer system cycle form shown in figure 10 is typical of the equipment operation check lists that are maintained. They provide a combined check list and operational history compatible with the scheduled maintenance program. The data on these forms is incorporated into a summary log, which, in turn, permits the scheduling of maintenance requirements during reactor down periods.

3.8.1.1 Test Loop Scheduled Maintenance

To conform with the projected test loop maintenance schedule, shown in figure 8, a form providing the required operating history is completed each time the loop is used for performance of a test. The form includes all activities necessary to complete an operational cycle, and the cumulative cycles of operation for the test loop. This information is then used to establish when scheduled maintenance is required. Any maintenance performed, scheduled or the result of a malfunction, was recorded in a maintenance log. A summary of these records indicating when scheduled maintenance was performed versus the total operating cycles to date is shown in figures 11 and 12.

During this reporting period, malfunctions occurred in test loops 201-003 (at nine cycles) and 201-004 (at seven cycles) which necessitated repairs (see section 3.8.2.1). Scheduled maintenance was performed simultaneously with the repairs for these test loops.

3.8.1.2 Refrigeration System Scheduled Maintenance

The refrigeration system has operated for a total of 1753.0 hours (1603.9 hours during this reporting period) since the system was overhauled. Scheduled maintenance was performed in conformance with the projected maintenance schedule shown in figure 9, as much as practicable. The total operating time during a reactor test cycle approaches 570 hours rather than the 500 hours which was used in establishing the maintenance schedule; therefore, the time between the maintenance periods has been extended so as not to interrupt the test program.

A summary of the total operating time of each engine and an indication of the type of maintenance performed is shown in figures 13, 14 and 15.

The relatively short periods of operation between maintenance at the beginning of the summary was the result of freeze-out of helium contaminants in the engines during operation at higher temperatures.

When the engines were cleaned, each was disassembled, requiring the installation of both O rings and valve body gaskets. Each time this was performed, this scheduled maintenance requirement was considered fulfilled and a new period initiated.

The piston rods, which should normally be replaced at 1000 hours were removed and carefully inspected for indications of incipient failure and reinstalled when no such indications were observed. The decision to reinstall the piston rods and obtain additional service data was reasonable, considering that modifications to improve alignment and double aging to enhance the mechanical properties had been incorporated during overhaul.

The compressor and vacuum system used in the refrigerator are essentially industrial equipment designed for continuous operation with minimum maintenance. The history of the performance of these systems has verified this; therefore, no specific maintenance schedule has been developed and the manufacturer's recommendations have been adhered to.

3.8.1.3 Hydraulic Panel Scheduled Maintenance

The history of malfunctions and repair of the hydraulic panel was not maintained in a form that would permit development of a time or cycle dependent maintenance schedule. In addition, the malfunctions recorded appeared to be of a random nature implying that scheduled requirements could not be logically developed.

Failure in this system has not precluded performance of any scheduled test and repairs were made during operation.

The accessibility of this equipment for repair and the availability of redundant equipment indicated that the operation or maintenance of the system would not prevent continued test operation and no scheduled maintenance program was developed.

3.8.1.4 Carriage Scheduled Maintenance

The inspection and maintenance of the test loop carriages was performed as indicated in figure 16. No repairs were required during this reporting period.

3.8.1.5 Transfer Table Scheduled Maintenance

A summary of the scheduled maintenance of the transfer tables as projected in figure 9 is shown in figure 17. During this reporting period, inspection and adjustments were made but no repairs were required.

3.8.1.6 Access Valve Routine Maintenance

Operational logs established for conformance with routine maintenance schedules (figure 9) for the beam port and hot cave access valve equipment are shown in figure 18. During this reporting period, routine inspections were made, but no repairs were required.

3.8.2 Repairs And Adjustments

During this reporting period, a number of repairs and adjustments were required for the test equipment. Some of these repair efforts were a continuation of effort previously reported (ref. 1) and some were required due to equipment malfunction during performance of the test program.

3.8.2.1 Test Loop Repairs

At the beginning of this reporting period, test loop required repair was in progress for test loops 201-002 and 201-003 and the three irradiated head assemblies 201-007, 201-008, and 201-010. During the reporting period, additional repairs were required on test loops 201-003 and 201-004. These problems are discussed in the following sections.

3.8.2.1.1 Test Loop 201-002

As previously reported (ref. 5), leakage in one of the helium refrigerant lines was evident in loop 201-002. The leak, as located, apparently exists in the aft welded weld joint of an expansion bellows incorporated in the inner tube of the double walled helium refrigerant line. During this reporting period, a suitable method of repairing the leakage was sought.

The use of a silicone sealant was tried using a test fixture with an intentional leak. The leak was not sealed in the test fixture, when evacuated, so the application of a sealant was not considered suitable.

The possibility of cutting a window into the outer shell of the test loop, as well as the outer line, is now being studied. For such a method to be feasible, the leak would necessarily need to be isolated and in such a location that the other transfer line would not interfere with repair efforts. To date, the leak has not been isolated to the extent required to provide assurance of an effective repair.

3.8.2.1.2 Test Loop 201-003

As reported previously (ref. 5), test loop 201-003 is known to have minute leaks in the actuating rod bellows assembly. This leakage has not prevented the use of this test loop for in-pile testing and repairs will not be undertaken until the leakage prevents accomplishment of test program objectives.

During this reporting period, the loss of the load transducer signal was observed in loop 201-003 during the ninth cycle of operation. The test loop was removed from the quadrant and transported to the hot laboratory work area to determine the cause of the malfunctions and to effect the necessary repair.

The malfunction indicated that water had entered the system and attenuated the signal which caused the failure. Upon inspection, it was noted that the extensometer feed-through connectors were leaking. New feed-through connectors were installed and the integrity established by leak testing with a mass spectrometer helium leak detector.

This test loop was then returned to the containment vessel and repositioned in the quadrant for use in subsequent testing.

3.8.2.1.3 Test Loop 201-004

After completion of seven operational cycles during this reporting period and while using test loop 201-004 to perform a tensile test, an erratic signal was observed indicating the possibility of a loose coil in the LVDT load transducer.

This test loop was removed from the quadrant and transported to the hot laboratory work area where the load transducer was removed and checked for faulty operation. None was observed.

Additional checking then indicated an intermittent type fault in the dynamometer lead line in the test loop which is a similar indication to that caused by a loose coil in the LVDT. The line was repaired, the dynamometer replaced with a calibrated unit and the test loop reassembled.

The loop was then returned to the containment vessel and placed in the quadrant for use in the next scheduled test cycle.

3.8.2.1.4 Test Loop Head Assemblies

At the beginning of this reporting period test loop head assemblies 201-007, 201-008, and 201-010 were not usable due to leaks which had developed (ref. 5). Studies were underway to determine methods for repairing the leaks.

During this reporting period, test loop head assembly 201-010 was shipped to Lockheed-Georgia Company Nuclear Laboratories in Dawsonville, Georgia, for repair of the hole in the nuclear instrumentation tube. The hole was welded, but subsequent leak checking with water indicated a gross internal leak apparently at a connection between the nuclear instrumentation tube and the head assembly. This was probably caused by the welding in the nuclear instrumentation tube. The blank-off cup weld (ref. 5) appeared to be successful, however.

The indicated leaks did not warrant further efforts to repair the 201-010 head assembly and it was sectioned just forward and just aft of the bellows assembly in order to examine the bellows for a possible visual cause of failure as occurred in head assemblies 201-007 and 201-008. Visual examination of the 201-010 bellows showed some evidence of oxidation at several locations.

The cask containing the head assembly sections was returned to Plum Brook. The indicated corrosion occurring in the test loop head assembly indicates that further repair work on head assemblies 201-007 and 201-008 is not warranted.

3.8.2.2 Refrigeration System Repairs

As discussed previously in reference 5, the evacuated thermal insulating space in one set of flexible helium transfer lines was known to be leaking. The loss of the vacuum surrounding the inner line caused a heat leak into the lines far exceeding the permissible rate and also reduced the available refrigeration to a level where a test specimen temperature of 30°R could not be maintained in the test loop.

The transfer lines terminate in a thermally isolated enclosure containing refrigerant shut-off and by-pass valves normally used to isolate the test loop from the refrigerant stream and to permit circulation of the refrigerant in the transfer lines to maintain them at low temperature during specimen change-over. These valves, in all three transfer line assemblies, have frequently malfunctioned or leaked so severely that they cannot be used for their intended application, thus requiring the utilization of manually operated valves in the manifold to isolate the test loops.

During this reporting period, a leak developed in the flexible line of another transfer line assembly at which time the manufacturer was contacted and arrangements were made for the repair and modification of the assemblies.

One assembly has been shipped to and received by the manufacturer. Repair and modification has been initiated with an anticipated completion date early in the next reporting period.

Inspection by the manufacturer of the first set of lines indicated that the valves may have been misaligned. The design is being changed to incorporate soft seats in the valves and also to allow the seats to be replaced without cutting or welding the valve chest assembly.

The extent and nature of the leaks in the transfer line vacuum space has not been repaired by the manufacturer.

The next assembly will be shipped to the manufacturer after the return of the initial assembly. The last assembly will be shipped after the return of the second assembly.

3.8.3 Corrosion of Test Equipment

A number of problems which came to light during the previous reporting period were attributed to corrosion (ref. 5). During this reporting period, additional evidence of corrosion was observed in the bellows of test loop head assembly 201-010 (see section 3.8.2.1.4). This problem is under study and corrective steps will be taken to alleviate the effect.

As discussed in detail in reference 5, the welded stainless steel actuator bellows assemblies which separate helium from cooling water in the test loops have exhibited serious corrosion at the welded peripheral seams. To alleviate this problem, the welded bellows in the test loops will be replaced by two sections of two-ply hydraulically formed bellows, welded end-to-end and welded to suitable adapters at the ends. The end-to-end welding is required because the section lengths are limited by the forming technique. The spring rate of the new bellows assembly is about 22 lb/in.

The first replacement is being made in the prototype loop to determine the best installation procedures before replacement of the bellows in the other loops. Following completion of this installation, the next replacement will be in test loop 201-005 which has not been irradiated so that assembly procedures can be perfected before working on an irradiated loop.

3.9 EXPERIMENT DESIGN MANUAL AND HAZARDS ANALYSIS

The changes in the Design Manual and Hazards Analysis required by the inclusion of cyclic tensile and compressive loading of the test specimen, previously discussed (ref. 5), were continued during this reporting period. These changes consist of design and operational modifications; fatigue testing will not increase operational hazard or compromise reactor safety. The revision of the Manual to include fatigue work shall be completed during the next reporting period.

As noted in reference 5, the possible hazard due to a sudden release of refrigerant gas was increased by the addition of in-pile operation at temperatures above 30°R. The initial Plum Brook Reactor Facility Safeguards Committee approval for insertion of the experiment into HB-2 was predicated on the assumption that the activation of the refrigerant was not a hazard since all gaseous impurities in the helium would be frozen out of the system at a heat exchanger located upstream from the expansion engines and test loop. Thus, during operations at 30°R, refrigerant contaminants would not enter the high flux zone of the experiment for activation.

The inclusion of irradiation exposures at 140°R, 320°R and 540°R in the test program will permit circulation of refrigerant contaminants through the activation zone. Since the refrigerant gas circulates through a compressor cycle located outside the controlled area of the containment vessel, and since the system is protected with relief valves and rupture discs which allow refrigerant gas release, an activation analysis of the refrigerant composition with a maximum impurity content was prepared. This was done to insure that no hazard to personnel exists, either inside or outside the containment vessel, in the event of the maximum credible incident.

3.9.1 Activation of Gases

The helium, as supplied, contains certain elemental H_2, Ne, N_2, O_2, and Ar; and C in the form of mixed oxides. The total weight fraction of impurity content is approximately 1.4×10^{-4}. The system also contains some air ($\approx$3.5 cc) entrapped at startup, although this is minimized by the system fill procedure. The total mass of entrapped air in the high flux zone is $\approx 4.5 \times 10^{-6}$ gms.

Since a part of the system is exposed to air by removal of the head assembly for each specimen change, consideration also needs to be given to this source of impurities in the helium stream. With the pump-down procedure used and with 144 specimen changes at intervals of fifteen hours, the total amount of air introduced is 1.7×10^{-6} cc, or approximately 2×10^{-9} gms. Thus, this source is negligible when compared with that introduced at system start-up.

The induced radioactivities depend only on the volume of the high flux zone (45 cubic inches), the gas density (from 0.038 lb/ft^3 at 540°R to 0.670 lb/ft^3 at 30°R), and the total system irradiation time between helium changes (60 days in-pile during a complete helium change every 90 days).

The maximum activity generated in the refrigerant gas is tritium, resulting from the H^2 (n, γ) H^3 (n,p) H^3 reactions. Ne^{23} from Ne^{22} (n, γ) Ne^{23} and Ar^{41} from Ar^{40} (n, γ) Ar^{41} reactions are also produced in significant quantities. All nuclear reactions, (n,α), (n, γ), (n, p) and (n, 2n) were considered for each isotope possibly present in the refrigerant, and those above were the only significant contributors to possible activity in the test loop.

The activation calculations were based on the equation:

$$N(t) = n \, \phi \, \sigma \, (1-e^{\lambda t})$$

When $N(t)$ = number of atoms of the radioisotope as a function of irradiation time, t.

n = number of parent atoms in high flux region.

ϕ = reactor flux

σ = cross section for given reaction in cm^2

λ = radioisotope decay constant

The maximum disintegration rates for the product radioisotopes from the significant reactions, together with the isotope half-life are given below:

Isotope	$T_{1/2}$	dis/sec
H^3	12.26 y	3.40 (+7) *
Ar^{41}	1.83 h	7.85 (+4)
Ne^{23}	38.00 s	6.60 (+3)

These activities were calculated on the basis of helium density at 140°R, the case in this test program providing the greatest mass flow and, therefore, the maximum exposure of parent isotopes to a high neutron flux.

3.9.2 Analysis of Hazards Due to Gas Activation

On the basis of the activation analysis briefly discussed in section 3.9.1, no appreciable hazard is presented by activation of gaseous impurities in the refrigerant.

---

* Numbers in parenthesis indicate power of 10.

The activity level of each of the significant isotopes is given below:

Isotope	Total Activity In System, μc	Activity Diluted To 8800 ft^3, $\mu c/cm^3$	MPC*, $\mu c/cm^3$ Controlled Area	Uncontrolled Area
H^3	9.43 (+2)	3.49 (- 6)	2.0 (-3)	4.0 (- 5)
Ar^{41}	2.12 (0)	8.50 (- 9)	2.0 (-6)	4.0 (- 8)
Ne^{23}	1.78 (-1)	7.15 (-10)	3.0 (-9)	1.0 (-10)

The activity is shown with the entire isotopic content in the system diluted to 8800 ft^3 since this represents the most severe credible gas release accident; instantanious release of all the refrigerant in this relatively small volume, approximately that of the compressor building.

Release of these radioactive gases to uncontrolled areas should present no hazard since under the worst conditions only one isotope has a concentration exceeding the uncontrolled MPC* while all the gas is still in the compressor building. A dilution factor of only 7.15 (dictated by Ne^{23}) is required by the time the radioactivity reaches an uncontrolled area to reach a level below the MPC. It should be noted that the activities are calculated without regard to the decay during circulation in the system or during release. The Ne^{23} has less than a forty second half life so that, in only a few minutes, it would decay to less than the uncontrolled area MPC. The system circulation period is several minutes.

Build-up of radioactivity through component leakage will not cause a hazard. The maximum allowable gaseous release from the compressor building is about 1 μc/min. The maximum activity generated in the refrigeration system is 943 μc of tritium. If this level of activity is present in the loop and since the normal system leakage into the compressor building is 4 ft^3/hr, then the activity release rate will be less than 0.1 μc/min:

$$943 \mu c \times \frac{4\ ft^3/hr}{1566\ ft^3} \times \frac{1\ hr}{60\ min} = 0.04 \frac{\mu c}{min}$$

Since tritium has a long half life, its build-up in the loop is proportional to the operating time and the activity will not reach 943 μc until near the end of the ninety day irradiation period.

*MPC - Maximum Permissible Concentration

Radiation exposure to personnel working near piping and equipment components containing helium and radioactive impurities presents no problem. The maximum dose rate that is tolerated for these conditions is 5 mr/hr. Using the approximate relationship that the dose rate at one foot is equal to six times the number of curies times the gamma energy in Mev, a curie value of 800 μc is obtained for a dose rate of 5 mr/hr at one foot from a 1 Mev gamma emitter. This is a factor of over 100 higher than the highest gamma activity (Ar^{41}) ever present in the loop.

For operation at temperatures above 140°R, the calculated activities would be reduced in the same proportion that the helium density is reduced, as by a factor of 0.27 at 540°R. At temperatures below 140°R the calculated activities would be increased but never by more than a factor of 4.79 (at 30°R). Inspection of the calculations shows that with this increase only the Ne^{23} and the Ar^{41} would be above the uncontrolled MPC, but argon is frozen out in the system before reaching the high flux region at all temperatures below 140°R, and neon freezes out below 44°R. At temperatures just above 44°R, the Ne^{23} in the compressor building would still require a dilution factor of less than thirty-five before reaching an uncontrolled area. Considering the short half life, the time required for release and the time required to reach an uncontrolled area, it is concluded that no hazard from induced gaseous activities at any possible operating temperature will exist.

These conclusions were included in the Experiment Design Manual and Hazards Analysis. This document was approved by the Plum Brook Reactor Facility Safeguards Committee and the experiment has been approved for operation at all temperatures up to 540°R.

4 TEST PROCEDURES

The test procedures discussed in the following sections are required for the acquisition of data under the carefully controlled test program environmental conditions and the reduction, analyses and interpretation of the data thus generated. Brief discussions of test specimen designs, flux mapping, tensile test methods, fatigue test methods, and post-exposure structural studies follow.

4.1 TEST SPECIMEN DESIGN AND FABRICATION

The test specimens used in this program are miniaturized due to various restrictions on the test equipment imposed by the nuclear cryogenic environment. Two specimen designs, one for the tensile test program and one for the fatigue test program, are required. The configuration of these test specimens is shown in figures 19 and 20.

4.1.1 Tensile Specimens

The tensile specimen shown in figure 19 and discussed in detail in reference 5, represents a miniaturization of the standard ASTM E-8 specimen (ref. 3). It is essentially a cylindrical tensile coupon two inches overall length, with threaded ends. The specimen gage length is 0.5 inch with a nominal diameter of 0.125 inch at the mid-point in the gage length, which conforms to the standard 4:1 gage length to diameter ratio. There is a slight taper to the mid-point of the gage length to insure fracture in that area.

Sufficient tensile test specimens have been fabricated for the current tensile testing requirements of this program with the exception of the annealing studies (section 5.1.1) added to the test program during this reporting period. The additional specimens needed are in the process of being fabricated.

4.1.2 Fatigue Specimens

Fatigue specimen design is not as standardized as tensile specimen design and the fatigue specimens to be used in this program will represent a departure from any commonly used design. However, the specimen geometric configuration is similar to that used by other investigators, such as Coffin (ref. 4). This will allow some degree of comparison between this data and data from other laboratories. During the previous reporting period (ref. 5), a preliminary specimen design was formalized and both analytical and experimental evaluations were initiated. The specimen design under investigation is shown in figure 20.

During this reporting period, low-cycle fatigue testing (using the preliminary control system described in reference 5) was conducted on several specimens of 18 Ni 300 Maraging Steel. Specimens were subjected to cyclic loading up to a maximum of 3300 pounds (approximately 270 ksi) alternately in tension and compression. The results are encouraging in that the failures (all in the tension half-cycle) occur after the approximate number of cycles expected based on the maximum load as a percentage of ultimate strength ($\approx$90%). No bending of the specimens has been observed even when the controls failed to stop the cycling and the specimen was joined and compressed to a high load after failure. One failed specimen (shown in figure 21) has been submitted to the NASA Plum Brook Hot and Metallurgical Laboratories Section for photographs and electron microscopy studies.

Thirty additional specimens, fifteen each of Aluminum 1100-0 and 18 Ni 300, aged, Maraging Steel, have been ordered from an outside manufacturer of test specimens for use in tests of fatigue test loop modification and procedures development. The Aluminum 1100-0, a commercially pure aluminum in the annealed condition, was selected as typical of the lowest strength materials (F_{ty}/F_{tu} ratio less than 0.5) likely to be encountered in any fatigue testing program. The 18 Ni 300 Maraging Steel, in the aged condition, was selected since the mechanical properties of this material at room temperature approximate those of the high strength titanium alloys at 30°R.

4.2 FLUX MAPPING

Accurate knowledge of the fast flux available in HB-2, both spectral shape and level, is necessary to determine the irradiation exposure required to provide the desired integrated flux for each specimen.

During this reporting period, flux mapping (required by a new gamma shield in the HB-2 beam port) was completed, except for measurements of flux distribution within the test loop head. The foil data has been reduced and results have been compared with similar data obtained in a previous test program (ref. 1) using this reactor facility and test equipment.

4.2.1 Foil Measurements

Seven foil runs were made to determine the flux and energy spectrum as a function of reactor control rod bank position. The foils used are listed in table 1. The range of threshold energies is 0.45 Mev to 8.6 Mev, with appropriate cross sections as listed. In addition, cobalt and cadmium covered cobalt were included to determine ratios of thermal flux to fast flux to complement the spectral data obtainable from the other foils.

The results of the seven foil runs are plotted in the lower portion of figure 22 as flux $> E_T$ versus E_T (where E_T is the threshold energy defined in table 1). The following assumptions were made before drawing the spectral plots through the available data points:

(1) The uranium and neptunium results as obtained (by radiochemistry rather than by direct counting) are not particularly reliable.

(2) The results from the indium foils are somewhat in doubt because of limited experience and knowledge of this monitor and the likelihood of errors due to cadmium oxide contamination. (The value from this foil for run seven is off the scale shown.)

(3) The shape of the spectra should be nearly consistent; that is, independent of reactor power level or control rod position; but the low energy fluxes are more dependent on control rod position than the higher energy fluxes.

(4) Results from magnesium are consistently high due apparently to uncertainty in the cross section value which was used.

(5) Based on a large amount of unpublished flux mapping data obtained by NASA, Plum Brook, sulphur is the most consistent and reliable of the monitors used. (All plots are drawn through the sulphur data points.)

The upper termination of each plot of flux versus E_T represents a data point for flux $>$ 0.5 Mev per watt of reactor power versus rod position.

4.2.2 Comparison of New Measurements With Previous Measurements

The new measurements were made following installation of a new gamma shield in the HB-2 beam port. For comparative analysis of specimen test data previously obtained (ref. 1) and data to be obtained, it is necessary to establish an equivalent flux to be used for new data. The new shield introduced compositional differences in the attenuating media (the shield) as well as a different specimen position relative to the reactor core.

The mapping technique used for new measurements was the same as used previously with the exception that indium foils were used in place of previously used thorium foils. Also the new results for fission foils are based on chemical separation before counting, a different technique than used previously.

The upper portion (curve) of figure 22 shows the results obtained from the program and indicates that the flux$>$0.5 Mev per watt of reactor power varies from about 2×10^4 nvt with the control rod at seventeen inches (early in the reactor cycle) to about 4×10^4 nvt with the control rod at thirty-one inches (late in the reactor cycle) with a well pronounced knee in the plot at about nineteen inches.

The new flux mapping data show only a minor difference, if any, between the new data and that from flux mapping in the earlier program. Any new plot showing monotonicly increasing flux versus rod position through the 0.5 Mev points indicated (by plus signs) would fall within plus or minus fifteen percent of the old plot. This is the range generally required to include ninety-five percent of all measurements that would be made by the best flux mapping techniques in a particular facility and location. Therefore, it cannot be concluded that there is a real difference.

The plot of flux$>$0.5 Mev per watt of reactor power versus control rod position, as shown in the upper part of figure 22, will be used to calculate exposure times for the current test program. No additional foil measurements will be made with the exception of intended measurements of flux distribution within the test loop head, unless changes in lattice configuration, fuel loading or experiment location indicate the possibility of significant shift in flux level or spectral shape.

The results of the new mapping indicate that the calculated fluxes for specimens irradiated are possibly somewhat low at the low rod positions and high at the high rod positions. The test results will be carefully analyzed as the program proceeds for any apparent correlation between differences in test values for particular materials, test conditions, and the control rod position. Sufficient mechanical property data has been accumulated so that variations in these properties at a particular test condition are possibly a better indication of error in calculated fluxes than actual flux measurements.

The results from the cobalt and cadmium covered cobalt indicate that the ratio of thermal flux to fast flux ($>$0.5 Mev) is approximately the same as before (0.33).

Gamma flux has not been measured, but indications (based on heat balances) are that it has increased by a factor of 1.5 to 2.0 with the new gamma shield, so that it is now about 0.2 per gram at the specimen location.

4.3 TENSILE TEST METHODS

Tensile testing requires the measurement and recording of several data for post-testing evaluation. These data include:

- Measurement and recording of the load on the specimen continuously from the initial application until specimen failure.

- Measurement and recording of the elongation of the specimen continuously from initial application of the load until a point after the total elongation represents more than 0.2% permanent strain.

- Measurement of specimen temperature throughout irradiation and testing.

- Measurement of elongation (a measure of total permanent strain) and reduction of area (a measure of non-uniform strain) on failed specimens as a post-irradiation examination.

The test methods required to provide accurate records of these parameters have been discussed in some detail in a previous report (ref. 5). A brief summary of these methods will be included in the following section, with a more detailed discussion of the specimen temperature control development work conducted during this reporting period.

4.3.1 Load-Strain Measurement and Recording, Data Reduction, Ductility Measurements

Load measurements are monitored with a ring type dynamometer, using a linear variable differential transformer (LVDT) to measure the ring deflection resulting from the applied load. Elongation is measured using an extensometer in which a LVDT measures the incremental separation between two knife edges initially 0.50 inch apart on the gage length of the specimen.

For load-elongation recording, the monitoring instruments convert the load or elongation into electrical signals, of which the strength is a function of the magnitude of the measured parameter. The electrical impulse from each of these instruments is amplified and plotted automatically by an X-Y recorder. Load appears as the Y plot, elongation as the X plot and the resultant load-elongation and the resultant load-elongation curves are recorded on graph paper as a permanent record of these test data. The extensometer is capable of measuring only about 0.010 inch elongation with reliable accuracy. After this limit of approximately 2% total strain has been reached, the recorder is switched to a load-time plot traveling at a rate of 0.02 in/sec.

The load-elongation curve developed during testing on the X-Y recorder and the initial specimen dimensions provide data for the determination of the ultimate tensile strength (F_{tu}) and the tensile yield strength (F_{ty}). The modulus of elasticity may be approximated from these curves, but an exact determination of this value is unobtainable due to the method of extensometer installation imposed by the necessity of using remote handling techniques.

Elongation and reduction of area values are obtained by fitting the broken specimens together and measuring the fractured gage length and minimum diameter by means of a micrometer stage and hair line apparatus accurate to $\pm$ 0.0001 inch. These values are reported as the change in magnitude from original specimen dimensions expressed as a percentage of the original value.

All of these methods conform to the requirements of ASTM Specification E-8 (ref. 3), with an extensometer installation classification of B-2 under ASTM Specification E-87 (ref. 3).

4.3.2 Specimen Temperature Control

Test specimen temperature control is required for three different test conditions: (1) expose and fracture at specified temperature without intervening warm-up, (2) expose at 30°R followed by warming to and fracture at higher temperature, and (3) expose at 30°R, anneal at a higher temperature and fracture at 30°R.

The direct measurement of these temperatures using thermocouples or other temperature measuring transducers was not considered practicable when performing a series of these tests (ref. 1). An alternate method of establishing the temperature at the specimen was incorporated into the refrigerator. This involves measurement of the temperature at the manifold inlet and return using platinum resistance type thermometers. These temperature measurements together with the return manifold sensor temperature establish the operational characteristics of the refrigerator permitting the determination of performance parameters which are related to the specimen temperature.

Temperature control conditions (1) and (2) were under investigation at the beginning of this reporting period, and partial results were previously reported (ref. 1). Temperature control condition (3) was added to the program during this reporting period.

4.3.2.1 Steady-State Temperature Control Condition

The nearly steady-state temperature control condition is defined as that condition for exposing and fracturing the test specimen at a controlled temperature without change of temperature between completion of exposure and tensile fracture. Four levels of temperature control (30°R, 140°R, 320°R and 540°R) are required in the performance of the tensile test program.

To determine the test specimen temperature during the performance of both in-pile and out-of-pile tests at designated temperatures, the program as previously described (ref. 5) was continued.

The copper-constantan thermocouple instrumented Ti-6Al-4V specimen was installed in the test loop and the temperature of the specimen was established at or near the test temperature and the operating parameters of the refrigerator were recorded. The latter included expansion engine pressure ratio, engine rpm, heat loads, loop inlet temperature, loop return temperature, and the return manifold temperature. Multiple runs were made at each test point of both the in-pile and out-of-pile tests to corroborate initial (ref. 5) data.

The results of these latest runs are shown in tables 2 and 3 which also indicate temperature gradients existing in the specimen. These results reflect the increasing ΔT characteristic between the engine exhaust temperature and return manifold sensor temperature, associated with maintaining the specimen at the high test temperatures, i.e., 140° and 320°R. They also indicate the effect of the in-pile gamma heating of the specimen and material within the thermally isolated enclosure.

Operational conditions predicated upon the return manifold sensor temperature have been developed to expand the operational range in the higher operating temperatures. These provide sufficient latitude to permit single pod operation, thus permitting continued operation in the event of a component failure in one engine pod.

The tests performed at 540°R provided sufficient data to indicate that the system will provide substantially more refrigeration than required for dissipating the gamma heat load. However, the progressive change in expansion engine performance caused by accumulation of helium contaminants presented variation in the data obtained and it is not shown in the tables. The wattage applied to the main line heater was in excess of 1000 throughout the test and the ΔT across the test loop was 35° to 40°R and the return manifold temperature was near or at ambient temperature. The system operated for over six hours before the accumulation caused engine stoppage.

Various methods of preventing the introduction of these contaminants into the expansion engines at the 540°R operature are currently being explored.

4.3.2.2 Temperature Control For Specimen Warm-Up

Part of the test program requires that the test specimen be maintained at 30°R throughout irradiation, but warmed to 140°R, 320°R or 540°R prior to fracture. The temperature-time relationships must be established for these test conditions.

The temperature-time relationship associated with specimen warm-up from 30°R to 140°R was recorded and the results reduced to provide the temperature-time history shown in figure 23. As indicated, the main heater wattage was increased to 2100 watts which exceeded the total refrigerator capacity, causing a time dependent temperature rise of the specimen. As the loop was retracted from the HB-2 beam port, eliminating the gamma heating, recorded temperature indicated a pronounced change in the loop return temperature, and as the engine rpm and main heater wattage were subsequently reduced to approximately the out-of-pile refrigeration requirements at 140°R, the temperature stabilized, maintaining the specimen at 140°R. A further reduction in the main heater load was effected to accommodate the slowly rising return manifold sensor temperature which ultimately would increase the loop inlet and return.

The latter reduction in heater load was apparently required to stabilize the system as the refrigeration resulting from the heat capacity of the system was approaching an equilibrium condition. Similar results will be obtained, as the program proceeds, for warm-up from 30°R to 320°R and from 30°R to 540°R and will be presented in later reports.

4.3.2.3 Temperature Control For Specimen Cool-Down

During this reporting period, the test program scope was changed to include isochronal annealing, i.e., irradiate at 30°R, warm to either 140°R, 320°R, or 540°R and anneal for one hour, then reduce the test specimen temperature to 30°R before fracture. The temperature-time relationships for the cool-down-following-anneal portion will be established, as the program proceeds, and reported in a manner similar to that for warm-up described in section 4.3.2.2 above.

4.4 FATIGUE TEST METHODS

After modification of test equipment (see sections 3.2.2 and 3.4) and determination of a suitable test specimen (see section 4.1.2), low-cycle fatigue characteristics of the selected materials will be studied. The test procedure will consist of applying a pre-determined stress load at a cyclic rate of 6 cpm for 10,000 cycles unless the test is interrupted before this point by specimen failure.

4.5 STRUCTURAL STUDIES

Structural studies are to be performed with the aid of optical microscopy, electron microscopy, and X-ray diffraction. Procedures for these methods are being developed in conjunction with NASA Plum Brook Reactor Facility personnel.

It is expected that transmission electron microscopy studies of the failed tensile specimens and electron fractographs of the fatigue specimens may be particularly valuable although both of these techniques present considerable difficulty, particularly in hot cell operations.

5 TEST PROGRAM

The initial scope of the test program, including the materials to be tested and the reasons for their selection, has been previously reported (ref. 5). Some modification of the program scope was made during this reporting period. These changes reflect the theoretical interest of polycrystalline high purity aluminum. Aluminum 1099-H14 is now to be tensile tested at 30°R after exposure at 30°R to lower total integrated fluxes, 5×10^{15} nvt (E>0.5 Mev) and 5×10^{16} nvt (E>0.5 Mev). Additional annealing studies, of an isochronal nature will also be conducted on Aluminum 1099. Since this material is of a limited engineering interest, Aluminum 1099 has been deleted from the fatigue portion of the testing program. The present scope of the program shown in tables 4 and 5, consists of the following major items:

- Effect of cryogenic-irradiation and annealing on tensile properties of pure aluminum (1099 Al).
- Effect of irradiation at 30°R on tensile properties of titanium and titanium alloys.
- Effect of irradiation at 30°R on low-cycle fatigue properties of titanium and titanium alloys.
- Effect of cryogenic temperature on tensile properties of commercially pure titanium and 7178 aluminum alloy.

All tests in the program are to be performed on specimens fabricated from materials manufactured using extraordinary precautions and provided with complete chemical and metallurgical pedigrees. A summary of the pedigree information is provided in tables 6 and 7.

During this reporting period, a total of seventeen specimens were irradiated during reactor cycles 39P, 40P, 41P, 42P and part of 43P. Two specimens were aborted (see section 3.2.1) and fifteen were tested from 4×10^{16} nvt to 1×10^{18} nvt (E $\geq$ 0.5 Mev). No out-of-pile tensile testing or fatigue testing within the scope of this program was performed during this reporting period.

5.1 TENSILE TEST RESULTS

The tensile testing portion of the program involves polycrystalline high purity aluminum, Aluminum 1099-H14, and three titanium alloys; Titanium 55A, Titanium 5Al-2.5 Sn, and Titanium 6Al-4V. During this reporting period, in-pile testing was started on Aluminum 1099 and all the in-pile testing of Titanium 55A was completed. The resultant test data is presented below. No out-of-pile testing was performed during this reporting period.

5.1.1 Aluminum 1099-H14

Tensile tests were performed on this material at 30°R after irradiation to 1×10^{17} nvt and 3×10^{17} nvt ($E > 0.5$ Mev) at 30°R. The partial test data is given in tables 8 and 9.

5.1.2 Titanium Alloys

Titanium 55A is the only titanium alloy tested during this reporting period. However, the in-pile tensile testing of this material was completed. The results are given in table 10 and figure 24. Figure 25 shows typical load-elongation curves for Titanium 55A in the various test conditions.

5.2 FATIGUE TEST RESULTS

No fatigue test results were obtained during this reporting period.

6 CONCLUSIONS

Complete tensile test results were available for only one material, Titanium 55A. This material, essentially unalloyed elemental titanium, showed a notable dependence of mechanical properties on irradiation level. The results of these tests are reported in section 5.2 and shown in tables 8, 9 and 10 and figures 24 and 25.

This material shows an irradiation level dependent change in mechanical properties at 30°R to flux levels of at least 10^{18} nvt (E>0.5 Mev). The strength functions show an increase proportional to fast neutron dose accompanied by a similar decrease in ductility functions. However, even at the highest exposure level, 10^{18}, there is adequate ductility for normal engineering applications.

7 REFERENCES

Reference	Source
1	Lockheed Nuclear Products: Effect of Nuclear Radiation on Materials at Cryogenic Temperatures. NASA CR-54881, 1966.
2	Lockheed Nuclear Products: Modification and Major Overhaul of Cryogenic Irradiation Facility at Plum Brook Reactor Facility. NASA CR-54770.
3	Anon: ASTM Standards, The American Society for Testing Materials, 1958, Part 3.
4	Coffin, L.F. Jr.; and Tavernelli, J.F.: The Cyclic Straining and Fatigue of Metals. Trans. Met. Soc. AIME, Vol 215, Oct. 1959, pp 794-807.
5	Lockheed Nuclear Products: Effect of Nuclear Radiation on Materials at Cryogenic Temperatures. NASA CR-54787, November 1965.

8 TABLES

TABLE 1 FLUX MAPPING FOILS

Type of Foil	Nuclear Reaction	Threshold Energy, E_T (Mev)	Cross Section ($\times 10^{-24}$ cm^2)
Indium	$In^{115}(n,n')In^{115\,m}$	0.45	0.20
Neptunium	$Np^{237}(n,f)\ Ba^{140}$	0.75	1.52
Uranium	$U^{238}(n,f)\ Ba^{140}$	1.45	0.54
Sulfur	$S^{32}(n,p)\ P^{32}$	2.9	0.284
Nickel	$Ni^{58}(n,p)Co^{58}$	5.0	1.67
Magnesium	$Mg^{24}(n,p)Na^{24}$	6.3	0.0715
Aluminum	$Al^{27}(n,\quad)\ Na^{24}$	8.6	0.23

TABLE 2 IN-PILE TEMPERATURE CORRELATION DATA

	Specimen Temperatures (°R)			Refrig. Temperatures (°R)			Heater Loads		Expansion Engine	
Test Run	Fwd.	Mid.	Aft	Loop Inlet	Loop Return	Return Manifold	Main (watts)	Trim (watts)	Pressure Ratio	Speed (RPM)
(30°R)										
1	30.4	29.9	30.3	29.1	32.3	32.3	200	40	6.1:1	325
2	30.7	30.3	30.6	29.0	32.6	32.6	200	25	6.0:1	320
3	30.4	29.8	30.2	29.1	32.5	32.5	200	30	6.1:1	320
(70°R)										
1	70.2	70.1	70.1	67.8	76.6	76.6	1200	20	6.1:1	325
2	70.4	70.3	70.1	67.3	77.1	77.0	1100	35	6.0:1	325
(140°R)										
1	140.0	139.6	139.8	136.2	150.5	150.0	1050	25	5.9:1	250
2	141.0	140.5	140.9	136.0	150.0	149.6	1100	5	6.0:1	250
(320°R)										
1	322.0	321.0	320.7	317.8	332.0	332.2	1300	70	6.0:1	250
2	320.5	319.6	320.1	318.2	331.7	331.8	1300	25	6.0:1	260

TABLE 3 OUT-OF-PILE TEMPERATURE CORRELATION DATA

	Specimen Temperatures (°R)			Refrig. Temperatures (°R)			Heater Loads		Expansion Engine	
Test Run	Fwd.	Mid.	Aft	Loop Inlet	Loop Return	Return Manifold	Main (watts)	Trim (watts)	Pressure Ratio	Speed (RPM)
(30°R)										
1	30.2	30.1	30.3	29.5	31.0	31.2	350	20	6.1:1	300
2	29.6	29.4	29.7	29.7	31.3	31.4	400	60	6.2:1	290
3	29.8	29.3	29.5	29.2	30.5	30.5	400	10	6.1:1	280
(70°R)										
1	70.3	70.1	70.6	68.0	72.1	72.0	1350	10	6.0:1	280
2	70.1	69.9	70.4	68.0	72.2	72.0	1250	60	6.2:1	270
(140°R)										
1	140.2	140.1	140.4	138.0	142.0	142.0	1600	35	6.1:1	260
2	140.6	140.4	140.8	138.5	142.7	142.5	1550	60	6.2:1	260
(320°R)										
1	320.1	320.1	320.2	318.1	322.3	322.0	1700	55	6.0:1	260
2	320.8	320.9	321.0	319.1	323.5	323.1	1650	25	6.0:1	270

TABLE 4 TENSILE TEST PROGRAM (SCOPE)

Material	Condition	Number Specimens	Exposure n/cm^2 (E 0.5 Mev)	Temperature (°R) Exposure	Temperature (°R) Post-Exposure	Remarks
1099 Al	-H14	3	5×10^{15}	30	--	(1)
1099 Al	-H14	3	5×10^{16}	30	--	(10)
1099 Al	-H14	3	1×10^{17}	30	--	(2) (9)
1099 Al	-H14	3	3×10^{17}	30	--	(9)
1099 Al	-H14	3	0	140	--	
1099 Al	-H14	3	1×10^{17}	140	--	
1099 Al	-H14	3	0	320	--	
1099 Al	-H14	3	1×10^{17}	320	--	
1099 Al	-H14	3	1×10^{17}	540	--	
1099 Al	-H14	3	0	30	140	(3)
1099 Al	-H14	3	1×10^{17}	30	140	(4) (10)
1099 Al	-H14	3	0	30	320	(3)
1099 Al	-H14	3	1×10^{17}	30	320	(4)
1099 Al	-H14	3	0	30	540	(3)
1099 Al	-H14	3	1×10^{17}	30	540	(4)
1099 Al	-H14	3	0	30	140	(5)
1099 Al	-H14	3	1×10^{17}	30	140	(6)
1099 Al	-H14	3	0	30	320	(5)
1099 Al	-H14	3	1×10^{17}	30	320	(6)
1099 Al	-H14	3	0	30	540	(5)
1099 Al	-H14	3	1×10^{17}	30	540	(6)
Ti-55A	Annealed	5	0	540	--	(7)
Ti-55A	Annealed	5	0	140	--	(7)
Ti-55A	Annealed	3	6×10^{17}	30	--	(8) (9)
Ti-55A	Annealed	3	1×10^{18}	30	--	(9)
Ti-5Al-2.5 Sn (ELI)	Annealed	3	1×10^{18}	30	--	(8)
Ti-5Al-2.5 Sn (STD)	Annealed	3	1×10^{18}	30	--	(8)
Ti-6Al-4V	Annealed	3	1×10^{18}	30	--	(8)
Ti-6Al-4V	Aged	3	1×10^{18}	30	--	(8)
7178 Al	-T651	5	0	540	--	(7)
7178 Al	-T651	5	0	140	--	(7)

(1). Data from tests at 30°R and 540°R without irradiation available from screening program (Ref. 1).

(2). Data from one specimen for this condition available from screening program (Ref. 1).

(3). Control specimen, to be stabilized at exposure temperature before stabilizing and testing at post-exposure temperature.

(4). To be stabilized at post-exposure temperature before testing at post-exposure temperature.

(5). Control specimen to be stabilized at exposure and post-exposure temperatures before stabilizing and testing at 30°R.

(6). Temperature to be reduced to and stabilized at 30°R before testing at 30°R.

(7). Data from five additional specimens available from screening program (Ref. 1).

(8). Data from tests at 30°R and 540°R without irradiation and at 30°R with 1×10^{17} n/cm^2 irradiation available from screening program (Ref. 1).

(9). These tests completed at the end of this reporting period.

(10). These tests partly completed at the end of this reporting period.

TABLE 5 -- FATIGUE TEST PROGRAM (SCOPE)

Material	No. Speci-mens (Max)	Test Type	Exposure °R	Exposure Cpm	Exposure Location
Ti-55A	9	Fatigue During Exposure	540	6	Out-of-pile
Ti-55A	9	Fatigue During Exposure	30	6	Out-of-pile
Ti-55A	9	Fatigue During Exposure	30	6	In-pile
Ti-5Al-2.5 Sn (Eli)	9	Fatigue During Exposure	540	6	Out-of-pile
Ti-5Al-2.5 Sn (Eli)	9	Fatigue During Exposure	30	6	Out-of-pile
Ti-5Al-2.5 Sn (Eli)	9	Fatigue During Exposure	30	6	In-pile
Ti-5Al-2.5 Sn (Std)	9	Fatigue During Exposure	540	6	Out-of-pile
Ti-5Al-2.5 Sn (Std)	9	Fatigue During Exposure	30	6	Out-of-pile
Ti-5Al-2.5 Sn (Std)	9	Fatigue During Exposure	30	6	In-pile
Ti-6Al-4V (Ann)	9	Fatigue During Exposure	540	6	Out-of-pile
Ti-6Al-4V (Ann)	9	Fatigue During Exposure	30	6	Out-of-pile
Ti-6Al-4V (Ann)	9	Fatigue During Exposure	30	6	In-pile
Ti-6Al-4V (Aged)	9	Fatigue During Exposure	540	6	Out-of-pile
Ti-6Al-4V (Aged)	9	Fatigue During Exposure	30	6	Out-of-pile
Ti-6Al-4V (Aged)	9	Fatigue During Exposure	30	6	In-pile

Material	No. Speci-mens (Max)	Test Type	Exposures nvt(E 0.5 Mev)	°R	Post-Exposure °R	Post-Exposure cpm
Ti-55A	9	Post-Exposure Fatigue	0	30	30	6
Ti-55A	9	Post-Exposure Fatigue	1×10^{17}	30	30	6
Ti-5Al-2.5 Sn (Eli)	9	Post-Exposure Fatigue	0	30	30	6
			(14 hr)			
Ti-5Al-2.5 Sn (Eli)	9	Post-Exposure Fatigue	1×10^{17}	30	30	6
Ti-5Al-2.5 Sn (Std)	9	Post-Exposure Fatigue	0	30	30	6
			(14 hr)			
Ti-5Al-2.5 Sn (Std)	9	Post-Exposure Fatigue	1×10^{17}	30	30	6
Ti-6Al-4V (Ann)	9	Post-Exposure Fatigue	0	30	30	6
			(14 hr)			
Ti-6Al-4V (Ann)	9	Post-Exposure Fatigue	1×10^{17}	30	30	6
Ti-6Al-4V (Aged)	9	Post-Exposure Fatigue	0	30	30	6
			(14 hr)			
Ti-6Al-4V (Aged)	9	Post-Exposure Fatigue	1×10^{17}	30	30	6

TABLE 6 MATERIAL COMPOSITION (PEDIGREE DATA)

ALLOY Temper	Lockheed Code	Al	Cu	Fe	Si	Mn	Mg	Zn	Ni	Cr	Ti
					Element Weight Percent						
Aluminum 1099 - H 14	8 Ba	99.99	0.003	0.001	0.001						
Aluminum 7178 - T 651	10 Ba	*	1.82	0.22	0.11	0.05	2.59	6.78	0.00	0.20	0.04

		Ti	C	Fe	Al	Sn	V		N_2	H_2	O_2
Titanium 55A Annealed	1 Aa	*	0.032	0.19					0.023	0.006	0.218
Ti-5Al-2.5 Sn (Std. I)	3 Aa	*	0.032	0.110	5.10	2.5			0.019	0.012	0.116
Ti-5Al-2.5 Sn (ELI) Annealed	8 Aa	*	0.033	0.028	5.43	2.41			0.011	0.0056	0.053
Ti-6Al-4V Annealed	2 Ac	*	0.010	0.170	5.95		4.00		0.022	0.006	0.065
Ti-6Al-4V Solution Treated and Aged	2 Aa	*	0.010	0.15	5.80		3.90		0.035	0.010	0.102

* Balance (by difference)

TABLE 7 MATERIAL PHYSICAL CHARACTERISTICS (PEDIGREE DATA)

Alloy / Temper	Lockheed Code	Form	Spec.	Vendor Code / Vendor Lot or Heat No.	F_{tu} (ksi)	F_{ty} (ksi)	Elongation (% in 4D)	Hardness	Grain Size ASTM No. (E112-58T)
Aluminum 1099 -H14	8 Ba	0.5" Plate	Vendor	199352 (1)	13.50*	12.90	20.5	Brinell	Not Measured
				199352	14.25**	13.95	19.5	26	
Aluminum 7178 -T651	10 Ba	1.0" Plate	Mil-A-	251777 (1)	89.55*	81.05	10.7	Brinell	Not Measured
			9180A	193-331	90.10**	80.80	10.7	168	
Titanium 55A Annealed	1 Aa	0.5" Round Bar	Mil-T-7993A Class II	(2) M-9186	70.5	60.5	35	Rockwell B 87	5
Ti-5Al-2.5 Sn (Std. I) Annealed	3 Aa	0.5" Round Bar	AMS-4910	(2) M-7888	131.0	127.0	22	Rockwell C 31-33	8
Ti-5Al-2.5 Sn (ELI) Annealed	8 Aa	0.5" Round Bar	Vendor 49021-1	(2) V-2402	119.3	101.2	17	Rockwell C 24.9	Not Measured
Ti-6Al-4V Annealed	2 Ac	0.5" Round Bar	Mil-T 9047C	(2) M8574	146.0	138.0	15.5	Rockwell C 30-33	Not Measured
Ti-6Al-4V Solution Treated And Aged	2 Aa	0.5" Round Bar	Mil-T 9047C	(2) M-9812	173.0	165.0	13	Rockwell C 33-36	Not Measured

* Longitudinal (orientation of test program specimens)
** Transverse

(1) Aluminum Company of America
(2) Titanium Metals Corporation of America

TABLE 8 PARTIAL TEST RESULTS, ALUMINUM 1099-H14

Specimen	Temp. (°R)	Irradiation (nvt, E 0.5 Mev)	F_{tu} (Ksi)	F_{ty} (Ksi)	F_{ty}/F_{tu}	Elongation (%)	Reduction of Area (%)	Fracture Stress (Ksi)	Modulus (x10^3 Ksi)
Mean of 5*	540	None	13.18	12.48	0.942	22.8	79.0	-	9
Mean of 5*	30	None	33.78	6.97	0.216	61.4	69.2	110.0	11
**	30	5×10^{15}							
**	30	5×10^{15}							
**	30	5×10^{15}							
Mean									
8 Ba 131	30	4×10^{16}	50.0	28.9	0.58	42	50	85.4	19
8 Ba 155	30	5×10^{16}	46.9	31.3	0.67	45	56	79.5	15
**	30	5×10^{16}							
**	30	5×10^{16}							
Mean									
8 Ba 87*	30	1×10^{17}	49.2	43.3	0.88	46	54	87.4	***
8 Ba 97	30	1×10^{17}	56.3	35.2	0.62	30	60	98.4	12
8 Ba 117	30	1×10^{17}	52.7	43.1	0.82	31	51	85.5	14
8 Ba 132	30	1×10^{17}	50.8	38.5	0.76	35	53	76.8	12
Mean	30	1×10^{17}	52.2	40.0	0.770	35.5	54.5	87.0	13
8 Ba 96	30	3×10^{17}	55.8	48.2	0.86	19	27	67.3	12
8 Ba 146	30	3×10^{17}	62.4	55.1	0.88	26	40	80.6	17
8 Ba 157	30	3×10^{17}	51.3	45.3	0.88	27	48	69.0	9
Mean	30	3×10^{17}	56.5	49.5	0.873	24.0	38.3	72.3	13

* From screening program (Reference 3)
\- Not available
** To be tested
*** Not determinable

TABLE 9 PARTIAL TEST RESULTS, ANNEALING AFTER IRRADIATION AT 30°R, ALUMINUM 1099-H14

Specimen	Annealing Temp. (°R)	Test Temp. (°R)	F_{tu} (Ksi)	F_{ty} (Ksi)	F_{ty}/F_{tu}	Elongation (%)	Reduction of Area (%)	Fracture Stress (Ksi)	Modulus ($\times 10^3$ Ksi)
Mean of 4*	Not Annealed	30	52.2	40.0	0.770	35.5	54.5	87.0	13
8 Ba 126	140	140	28.7	22.8	.79	29	61	-	-
**	140	140							
**	140	140							
Mean									
**	140	30							
**	140	30							
**	140	30							
Mean									
**	320	320							
**	320	320							
**	320	320							
Mean									
**	320	30							
**	320	30							
**	320	30							
Mean									
**	540	540							
**	540	540							
**	540	540							
Mean									
**	540	30							
**	540	30							
**	540	30							
Mean									

* From table 8
** To be tested
\- Not available

TABLE 10 TEST RESULTS, TITANIUM 55A (ANNEALED)

Specimen	Temp. (°R)	Irradiation (nvt, E 0.5 Mev)	F_{tu} (Ksi)	F_{ty} (Ksi)	F_{ty}/F_{tu}	Elongation (%)	Reduction of Area (%)	Fracture Stress (Ksi)	Modulus ($\times 10^3$ Ksi)
Mean of 5*	540	None	67.0	53.5	0.798	30.0	62.3	-	14
Mean of 5*	30	None	169.4	122.0	0.722	33.3	53.0	-	18
Mean of 3*	30	1×10^{17}	192.3	131.7	0.690	34.0	53.0	-	18
1 Aa 200	30	6×10^{17}	203	154	0.75	29	45	370	20
1 Aa 203	30	6×10^{17}	204	158	0.78	29	46	380	19
1 Aa 153	30	6×10^{17}	211	154	0.73	27	38	341	15
Mean	30	6×10^{17}	206.0	155.3	0.753	28.3	43.0	363.7	18
1 Aa 152	30	1×10^{18}	213	159	0.74	30	49	420	12
1 Aa 205	30	1×10^{18}	216	171	0.79	29	44	387	22
1 Aa 206	30	1×10^{18}	223	181	0.81	19	38	358	**
Mean	30	1×10^{18}	217.3	170.3	0.780	26.0	43.7	388.3	17

* From screening program (Reference 3)
\- Not available
** Modulus slope apparently in error

9 FIGURES

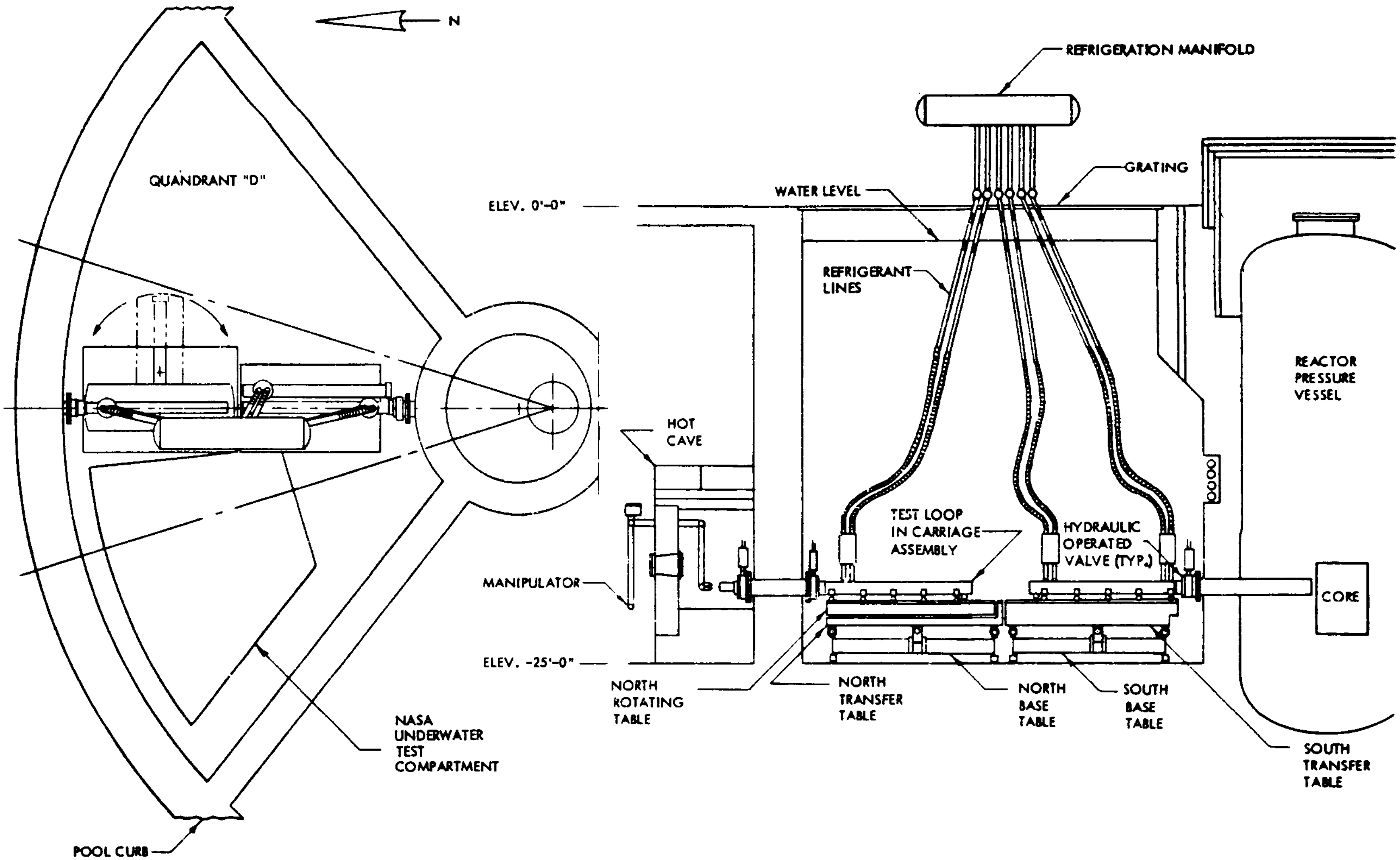

FIGURE 1 SYSTEM LAYOUT

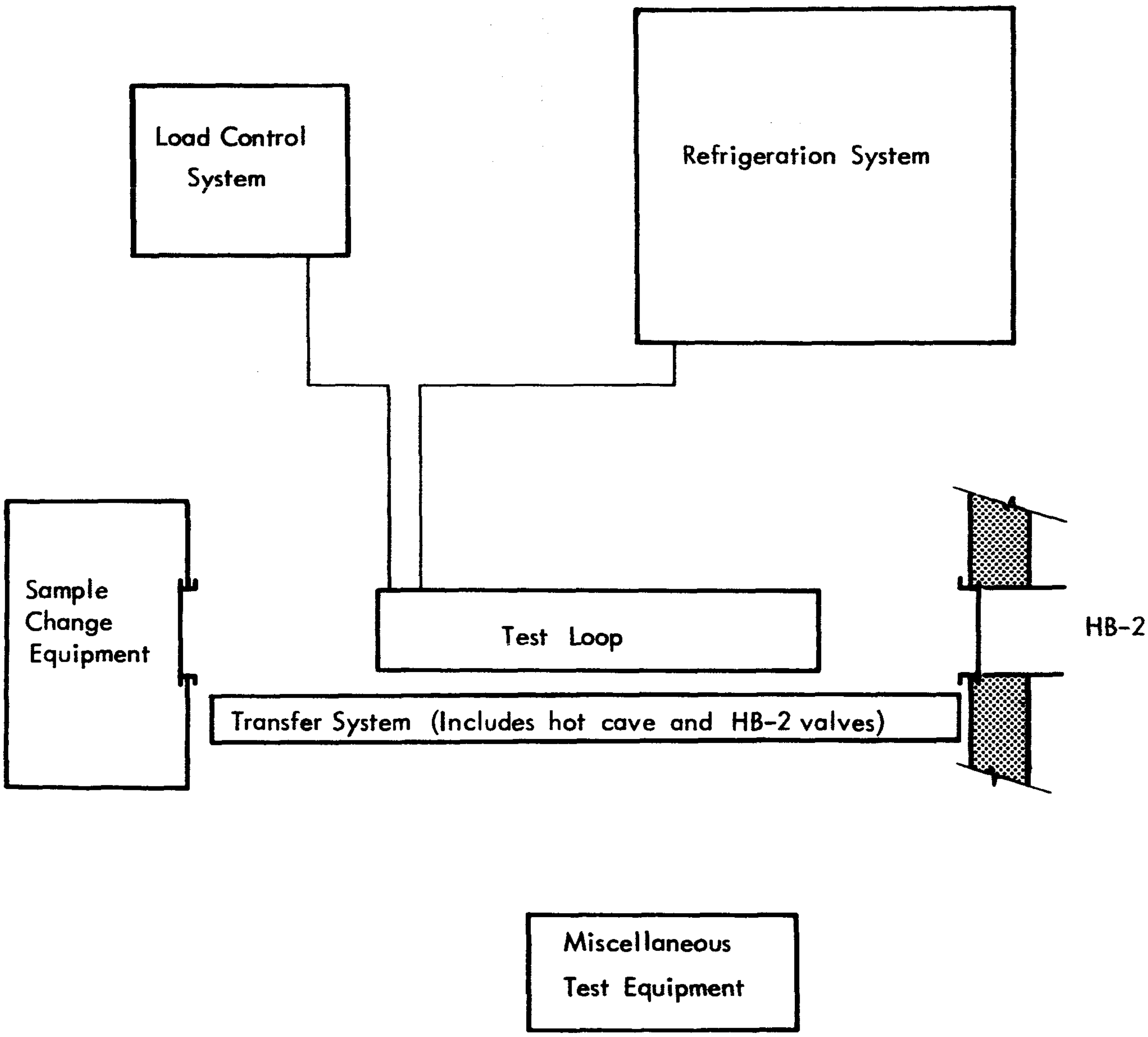

FIGURE 2 TEST EQUIPMENT (BLOCK DIAGRAM)

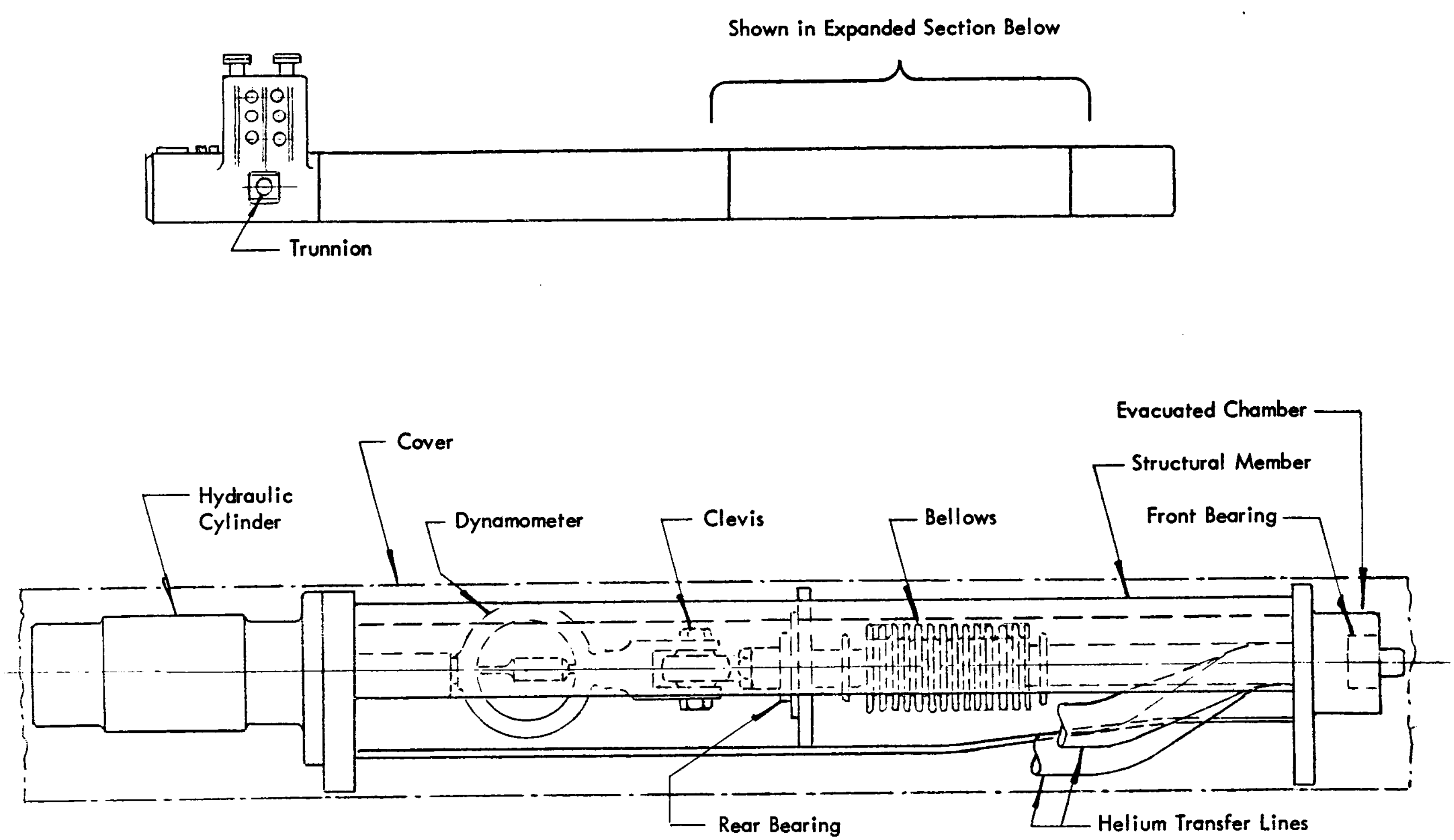

FIGURE 3 TENSILE TEST LOOP ASSEMBLY

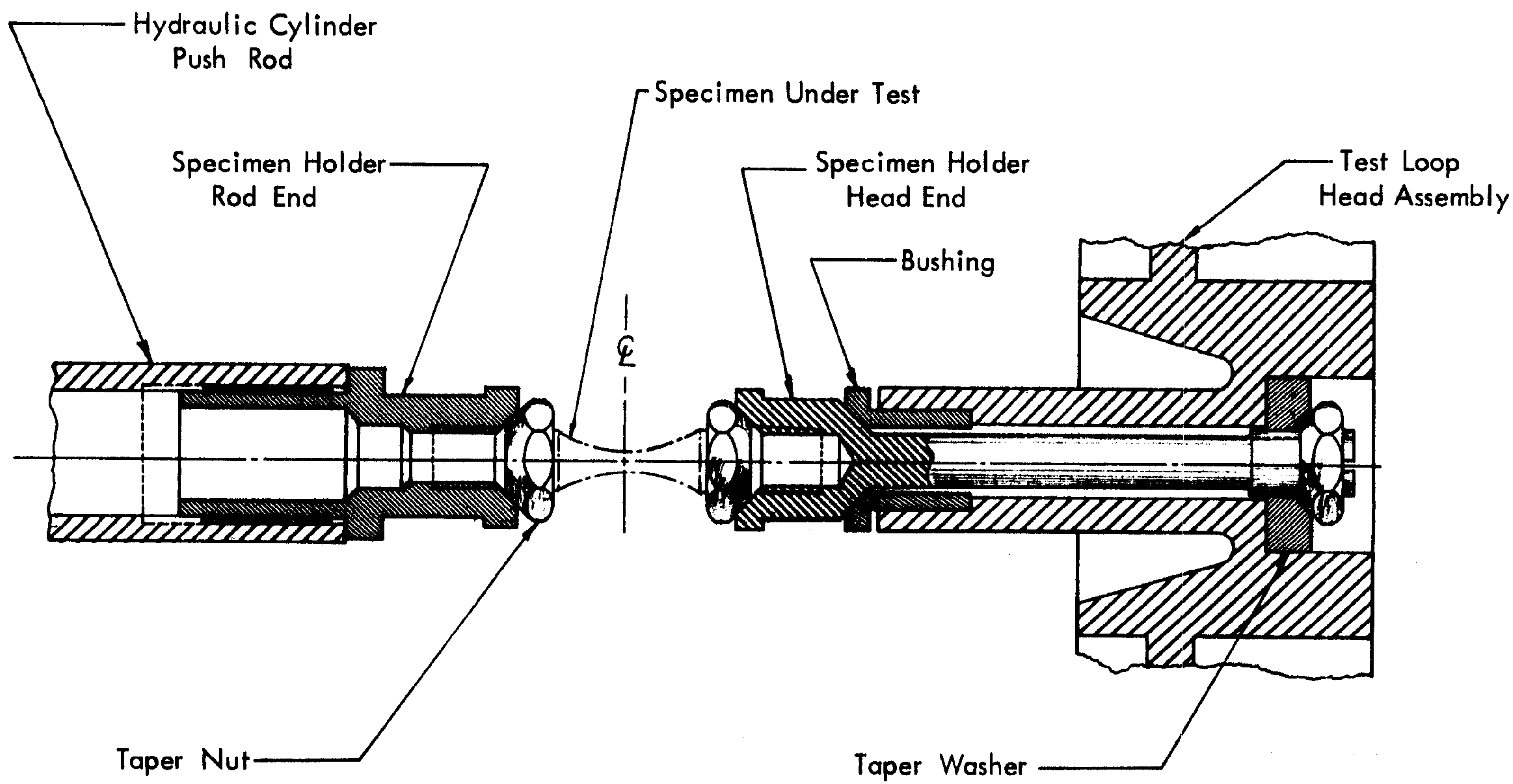

FIGURE 4 SPECIMEN HOLDER DESIGN

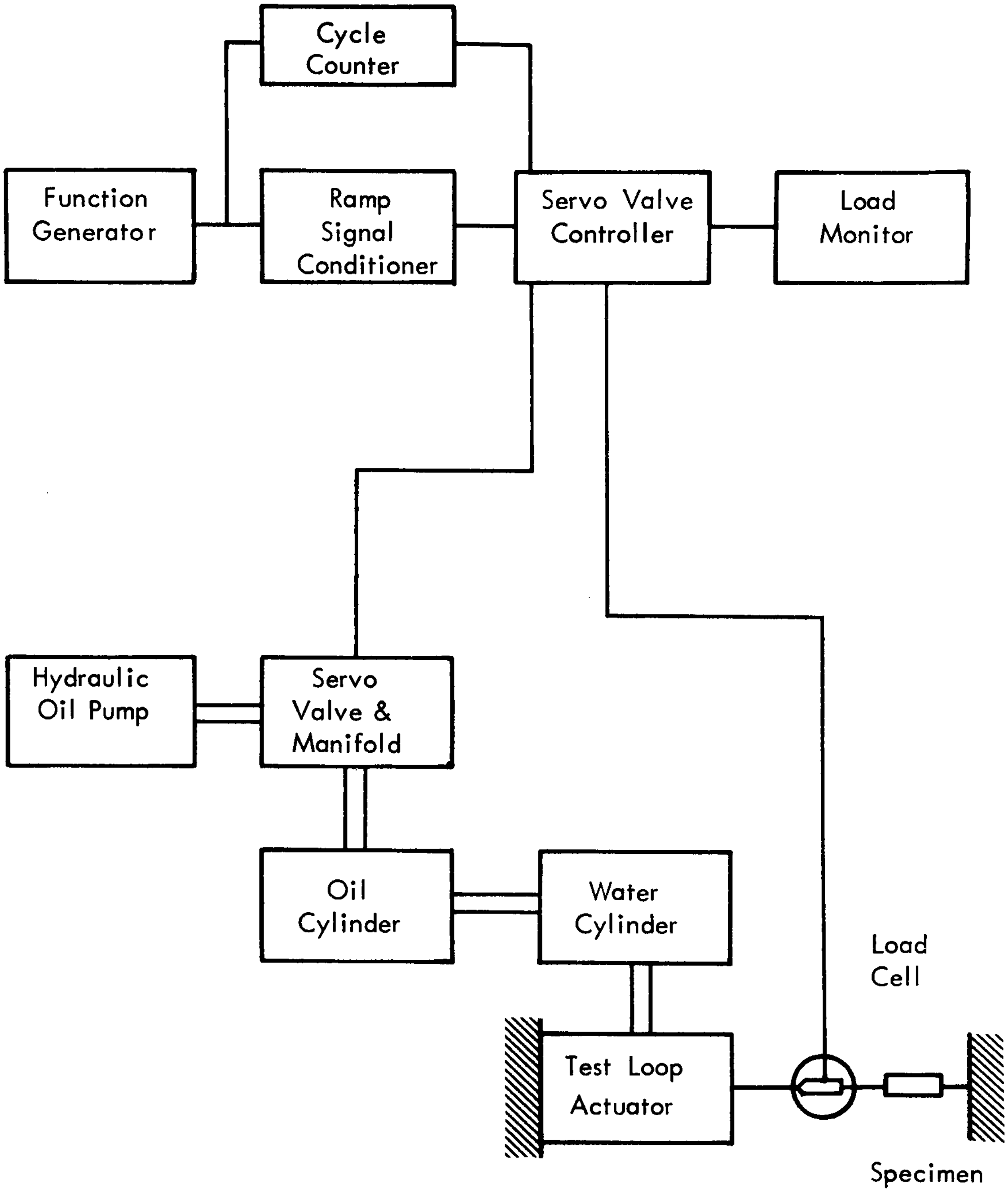

FIGURE 5 FATIGUE LOAD CONTROL SYSTEM (BLOCK DIAGRAM)

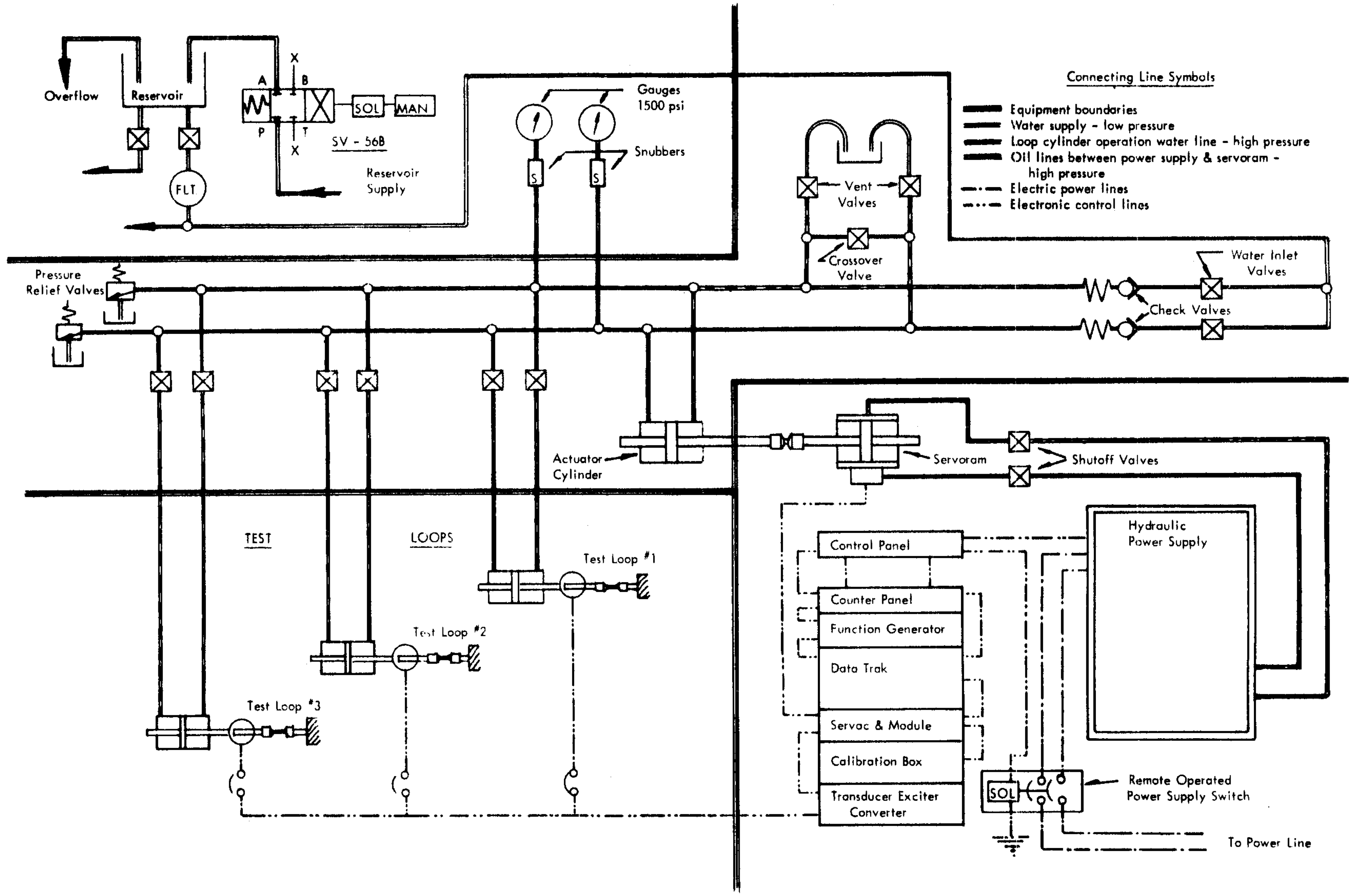

FIGURE 6 LOAD CONTROL SYSTEM (SCHEMATIC)

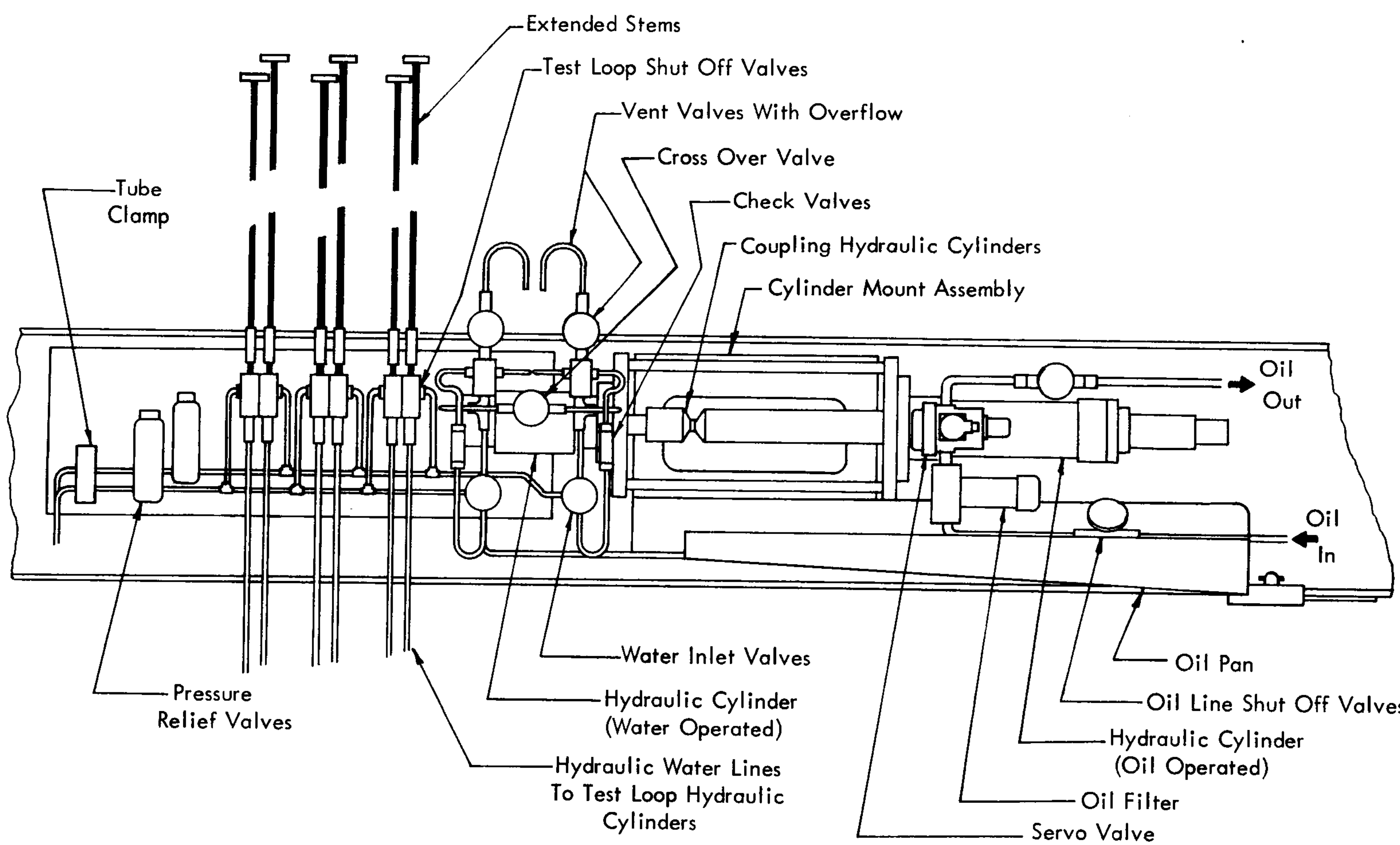

FIGURE 7 TEST LOOP ACTUATION CENTER

Cycles	0	5	10	15	20	25	30	35	40	45	50
TEST LOOP											
Instrumentation											
Calibration Load Transducer											▼
Electrical Integrity			▽		▽		▽		▽		▽
Extensometer		▼▼▼▼▼	......	......	......	......	......	......	......	......	......
Mechanical Integrity			▽		▽		▽		▽		▽
Pressure Integrity											
Refrigerator System-Helium											▽
Static Sumergence-Water											▽
Coolant System-Water											▽
Load Actuator Mechanism											
Dynamic Characteristics			▽ f		▽ f		▽ f		▽ f		⧩
Hydraulic Units (Mini Pump)			▽ f		▽ f		▽ f		▽ f		⧩
CARRIAGES											
Drive System			▽		▽		▼		▽		▽
Hydraulic Motor							⧩				
Drive Gearing			▽		▽		⧩		▽		▽
Drive Bearings			▽		▽		▽		▽		▽
Yoke Support Bearings			⧩		⧩		▼		⧩		⧩
Limit Switches			▽		▽		▽		▽		▽
TRANSFER TABLES											
Carriage Drive (Longitudinal)											
Hydraulic Units											▽
Stop System - Fixed											▽
Stop System - Hydraulic											⧩
Clutch Mechanism											⧩
Rack & Pinion Drive											▽
Limit Switches			▽		▽		▽		▽		▽
Transverse Drive											
Hydraulic Units											▽
Bearing Assemblies											▽
Stop System - Fixed											▽
Stop System - Hydraulic											▽
Limit Switches			▽		▽		▽		▽		▽
Rotational Drive (North Table)											
Stop System - Fixed							▽				
Limit Switches			▽		▽		▽		▽		▽
BEAM PORT AND HOT CAVE ACCESS VALVES											
Carriage Coupling Assembly											⧩
Seal Integrity											⧩
Primary Water Isolation System						▽					▽

▽ Inspection & Adjustment if Required

⧩ Disassembly and Inspection

▼ Replacement Overhaul

f Fatigue Equipment

FIGURE 8 TEST FACILITY EQUIPMENT MAINTENANCE SCHEDULE

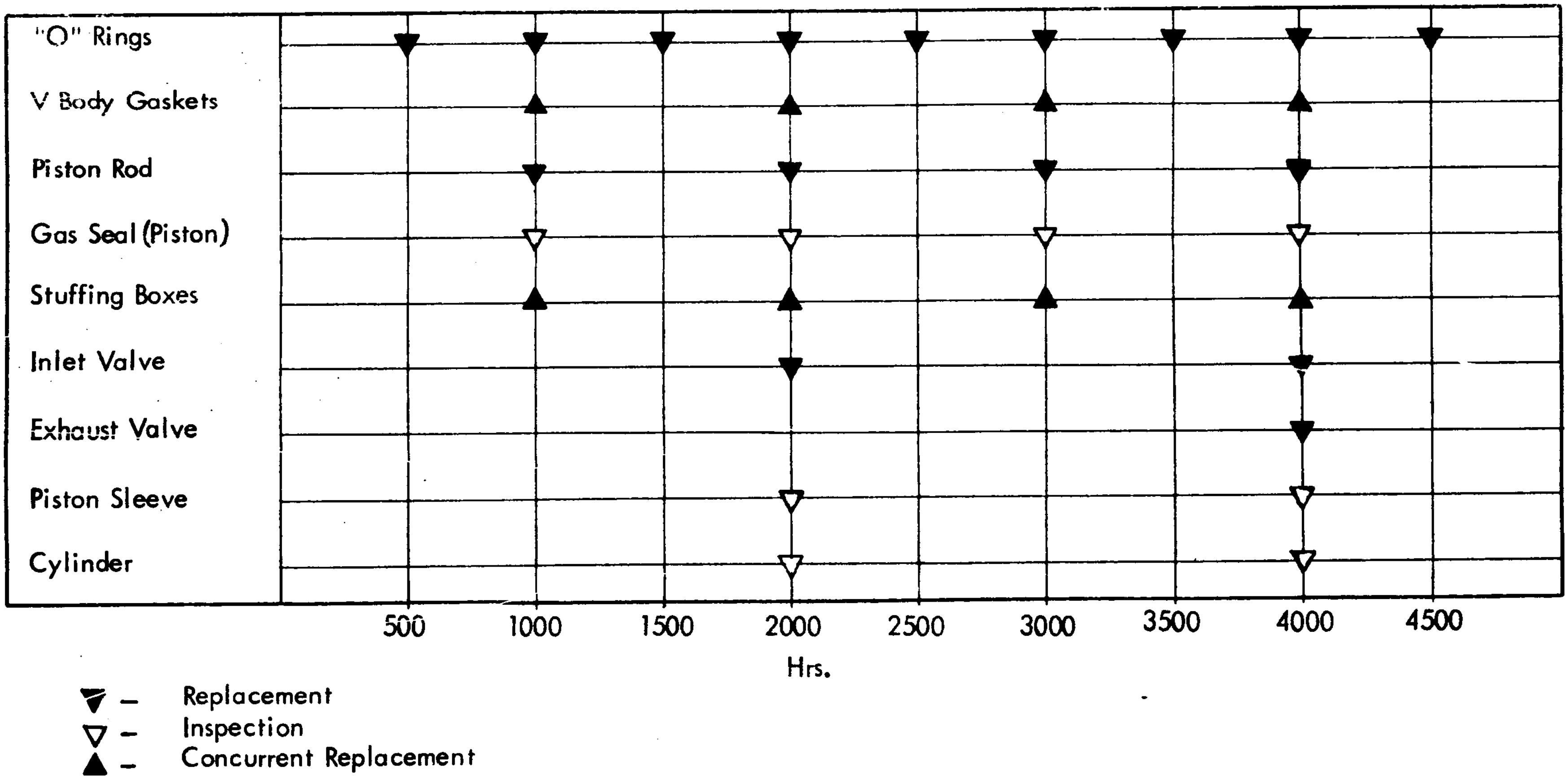

FIGURE 9 EXPANSION ENGINE MAINTENANCE SCHEDULE

TRANSFER SYSTEM CYCLE

LOOP NO.________________ CYCLES TO DATE____________

CARRIAGE NO.______________ CYCLES TO DATE____________

REACTOR CYCLE NO.________

HOT CAVE INSERTION CHECK LIST

DATE__________ TIME__________

"Reactor-Hot Cave" Switch in Hot Cave Position	☐	initial
"Master-Hot Cave" Switch in Master Position	☐	initial
Hot cave valve in quadrant open (visual inspection)	☐	initial
Communication between operators	☐	initial
"Master-Hot Cave" Switch changed to "Hot-Cave" position	☐	initial
Hot cave valve open - Verified	☐	initial
Insertion Complete	☐	initial
"Master-Hot Cave" switch returned to "Master" position	☐	initial

HOT CAVE REMOVAL CHECK LIST

DATE__________ TIME__________

Communication between operators	☐	initial
"Master-Hot Cave" Switch in "Hot Cave" Position	☐	initial
"Reactor-Hot Cave" Switch in "Hot Cave" Position	☐	initial
Hot cave valve closed	☐	initial
"Master-Hot Cave" Switch changed to "Master" Position	☐	initial
Hot Cave valve in quadrant in "closed" position	☐	initial
Loop "normal rear" position	☐	initial

BEAM PORT INSERTION CHECK LIST

DATE__________ TIME__________

Track position with respect to beam port	☐	initial
Sample Temperature a. Inlet helium temperature °F b. Outlet helium temperature °F	☐	initial
Check dynamic hydraulic pressure high range (550 psig)	☐	initial
Manual test loop cooling water valves open	☐	initial
Test loop cooling water Flow Verify	☐	initial
Seal water flow on	☐	initial
Seal water pressure, psi	☐	initial
Beam port valve position	☐	initial
Test loop position (full forward)	☐	initial
Time Insertion Complete	☐	initial

BEAM PORT REMOVAL CHECK LIST

DATE__________ TIME__________

Manual test loop cooling water valves closed	☐	initial
"Seal" light off	☐	initial
Beam port valve closed	☐	initial
Test loop cooling water flow off	☐	initial
Seal Water flow off	☐	initial
Test loop position (normal rear)	☐	initial
Time Withdrawal Complete	☐	initial

REMARKS: ____

FIGURE 10 TRANSFER SYSTEM CYCLE OPERATION FORM

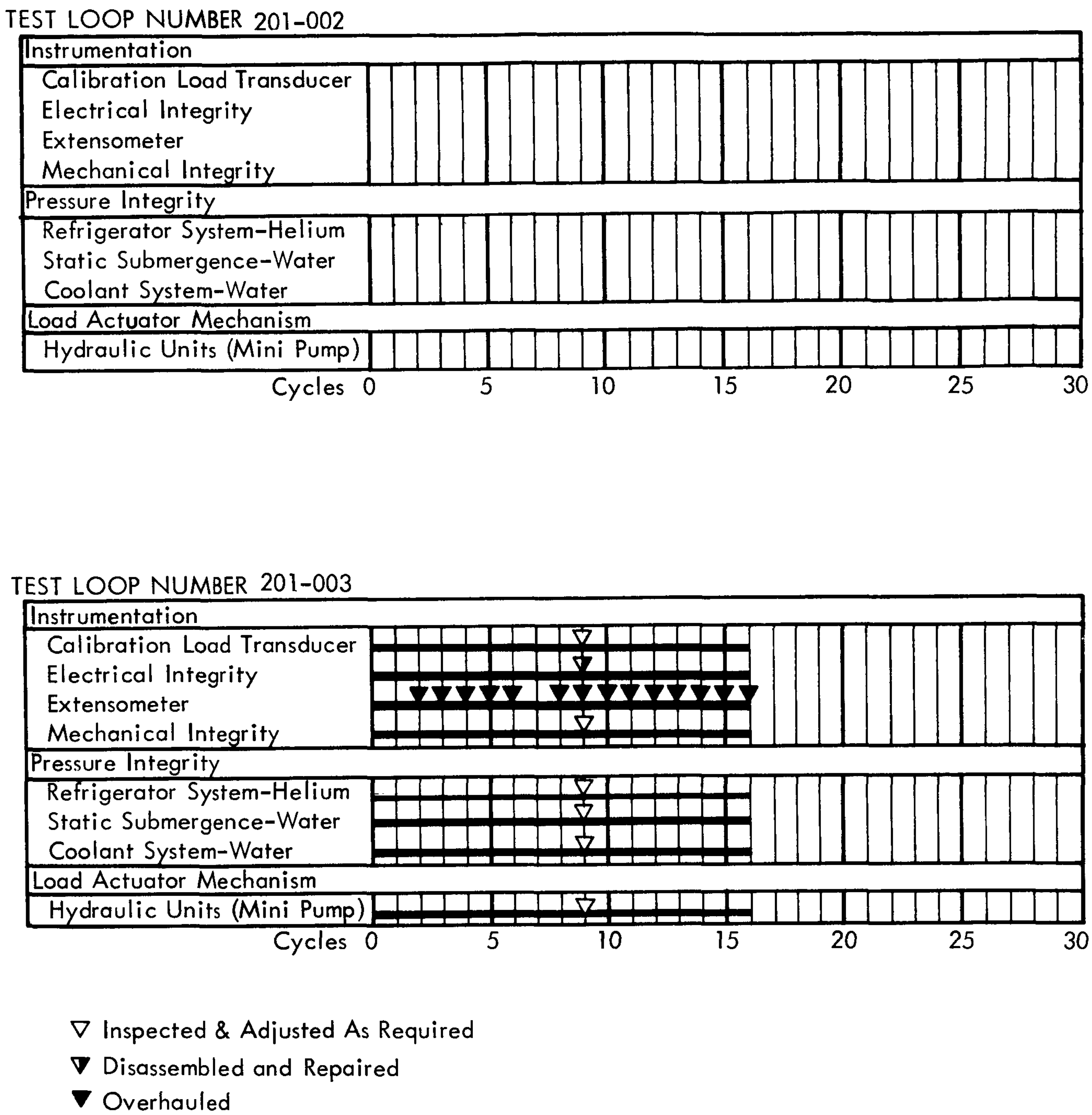

FIGURE 11 MAINTENANCE HISTORY - TEST LOOPS 201-002 AND 201-003

TEST LOOP NUMBER 201-004

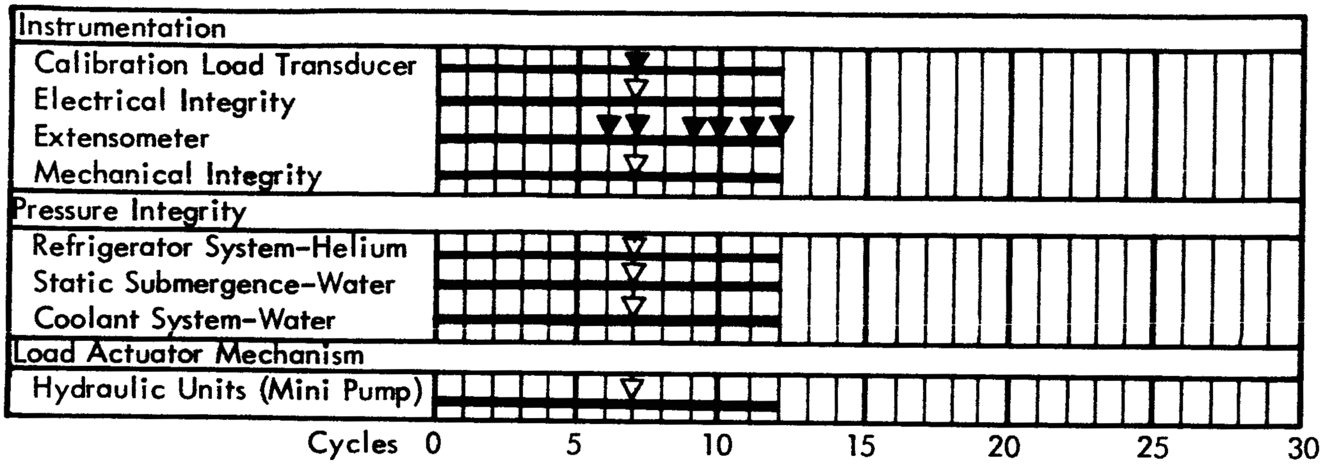

TEST LOOP NUMBER 201-005

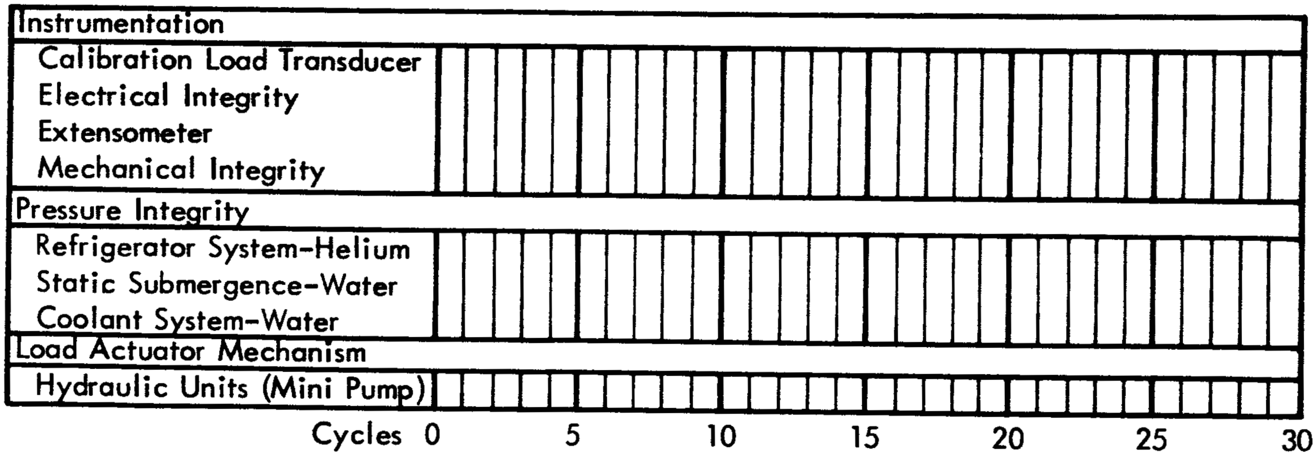

▽ Inspected & Adjusted As Required

▼ Disassembled and Repaired

▼ Overhauled

FIGURE 12 MAINTENANCE HISTORY - TEST LOOPS 201-004 AND 201-005

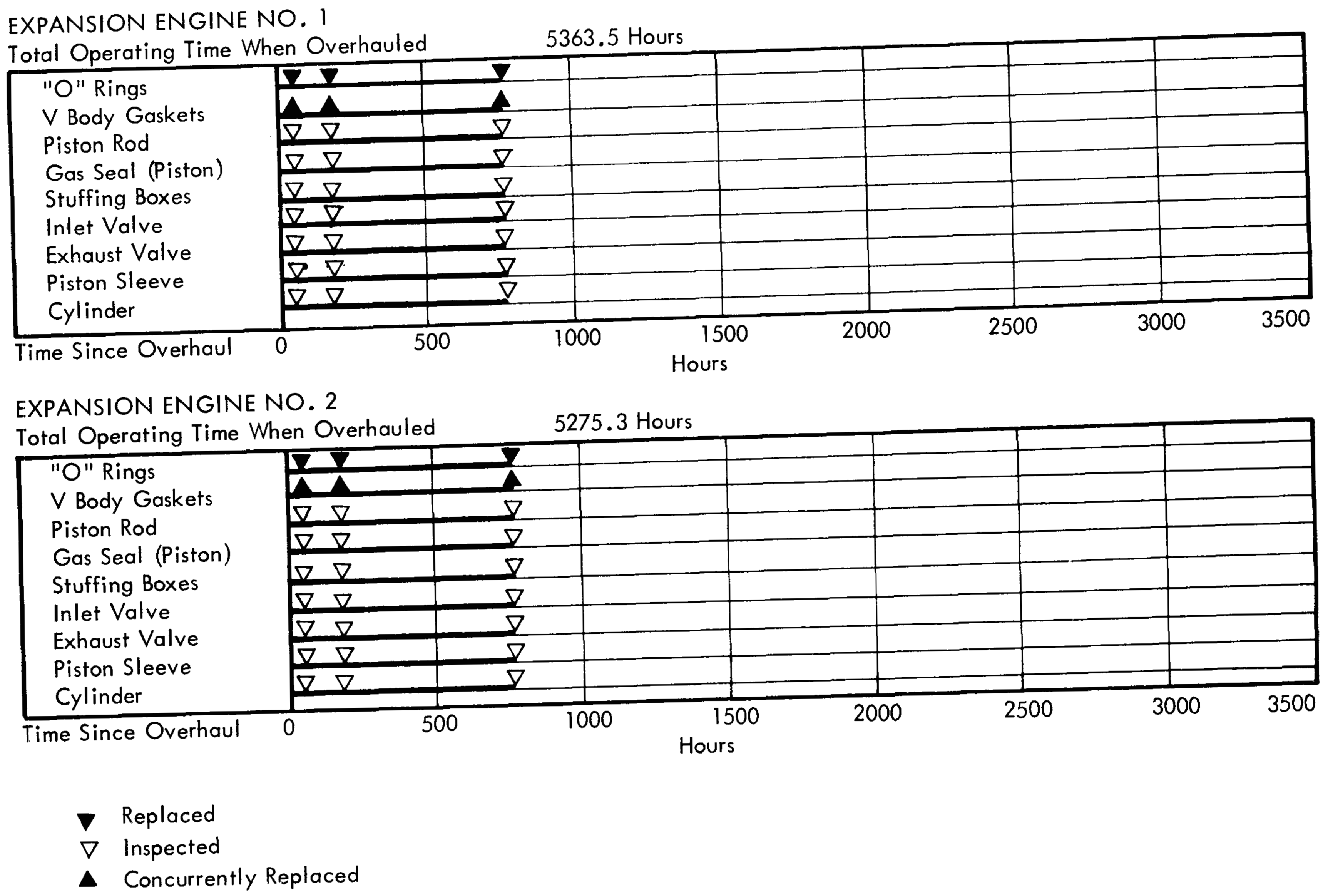

FIGURE 13 MAINTENANCE HISTORY - EXPANSION ENGINES NO. 1 AND NO. 2

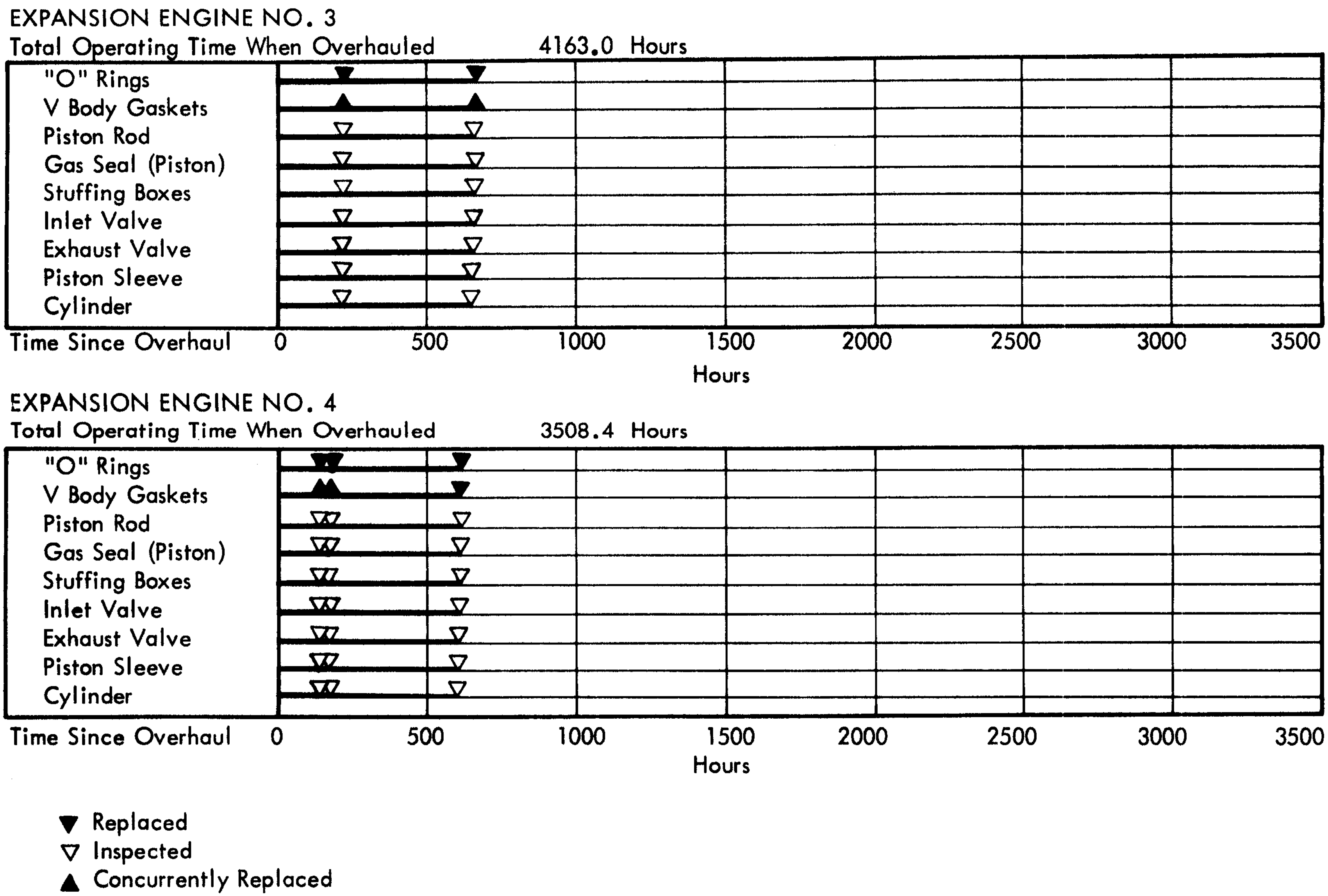

FIGURE 14 MAINTENANCE HISTORY - EXPANSION ENGINES NO. 3 AND NO. 4

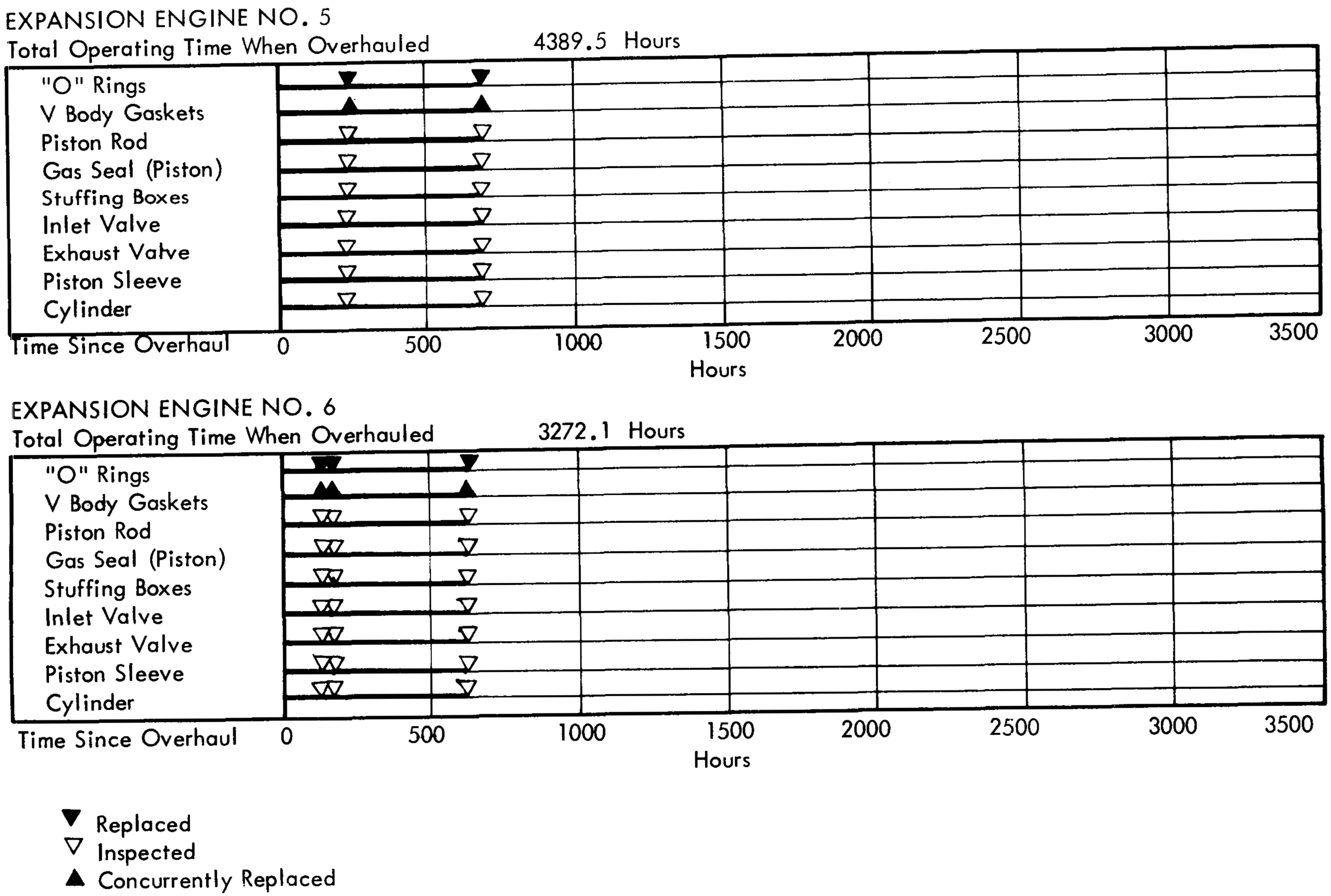

FIGURE 15 MAINTENANCE HISTORY - EXPANSION ENGINES NO. 5 AND NO. 6

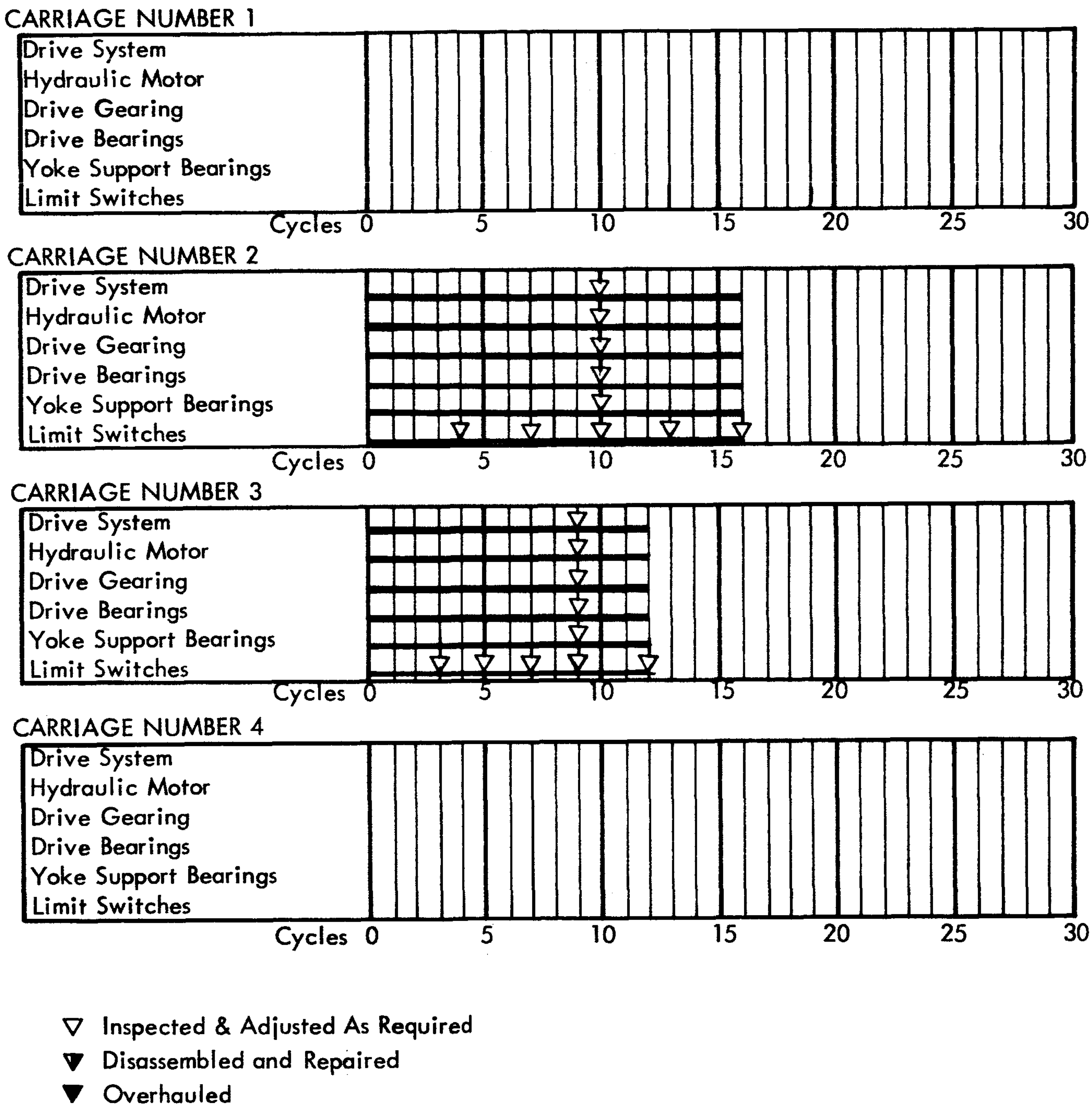

FIGURE 16 MAINTENANCE HISTORY - TEST LOOP CARRIAGES

SOUTH TRANSFER TABLE

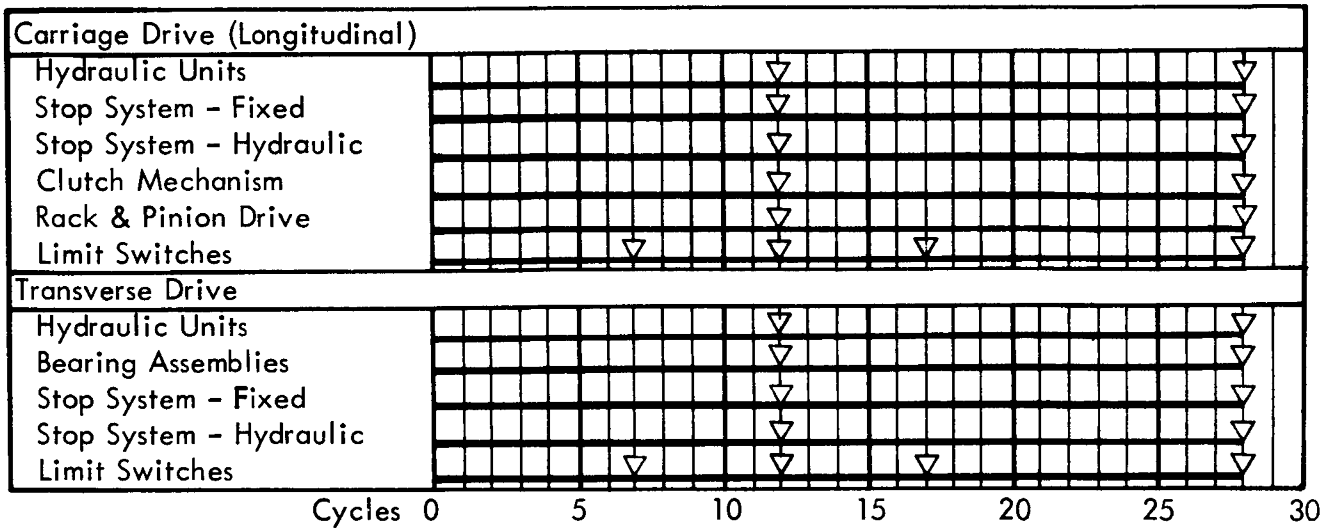

NORTH TRANSFER TABLE

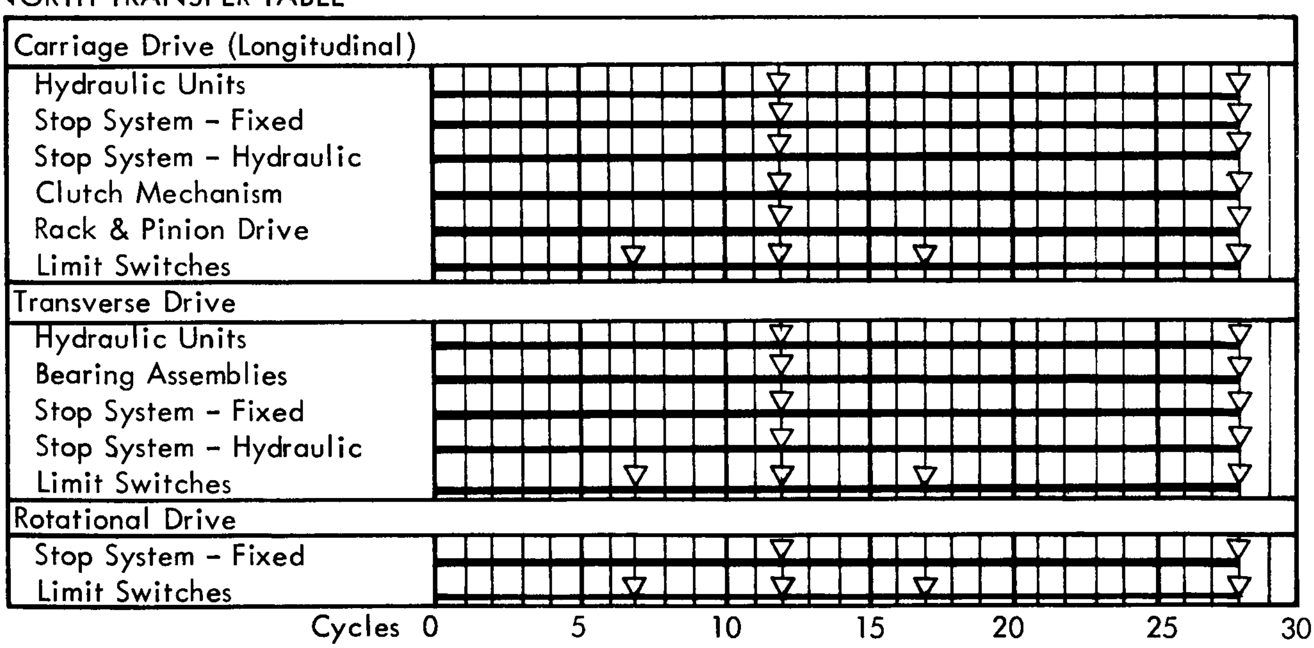

▽ Inspected & Adjusted As Required
▼ Disassembled and Repaired
▼ Overhauled

FIGURE 17 MAINTENANCE HISTORY - TRANSFER TABLES

BEAM PORT ACCESS VALVE
EQUIPMENT

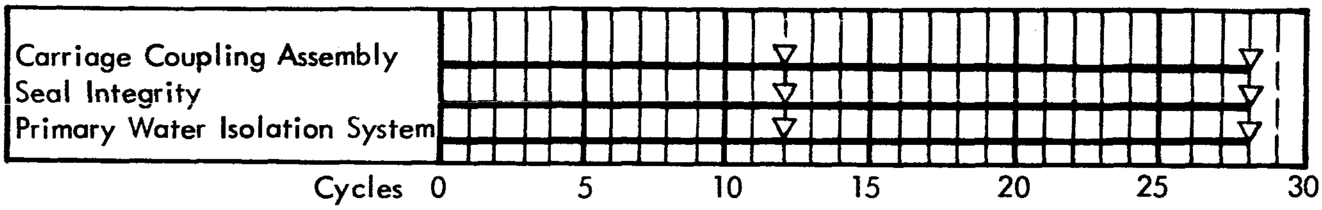

HOT CAVE ACCESS VALVE
EQUIPMENT

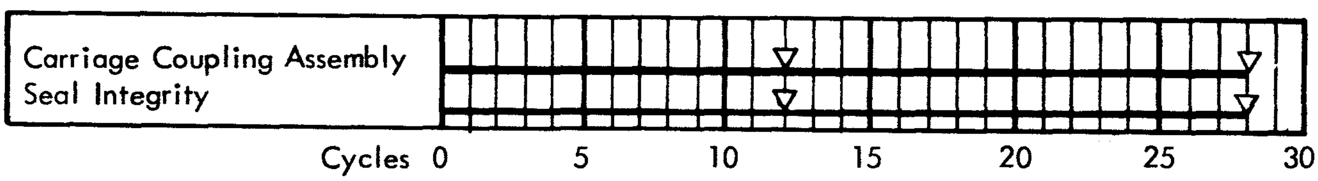

▽ Inspected & Adjusted As Required

▼ Disassembled and Repaired

▼ Overhauled

FIGURE 18 MAINTENANCE HISTORY-BEAM PORT AND HOT CAVE ACCESS EQUIPMENT

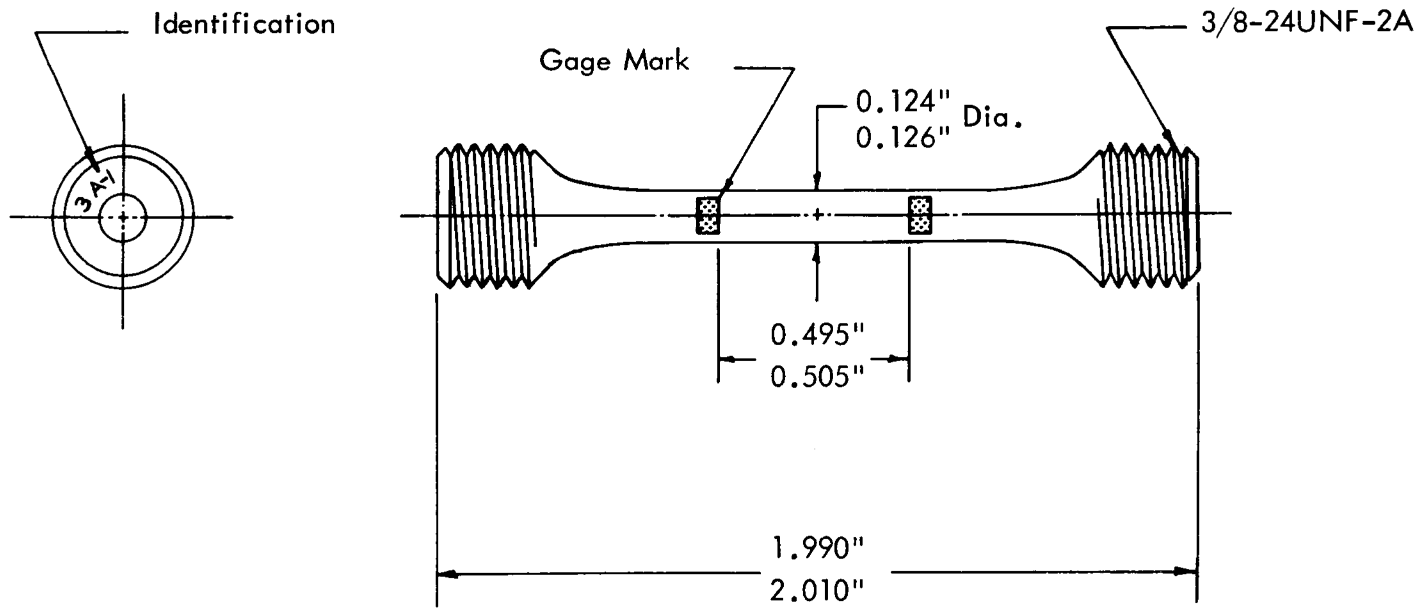

Note: Diameter at gage marks shall be center diameter + $\frac{0.002"}{0.004"}$.

FIGURE 19 TENSILE SPECIMEN

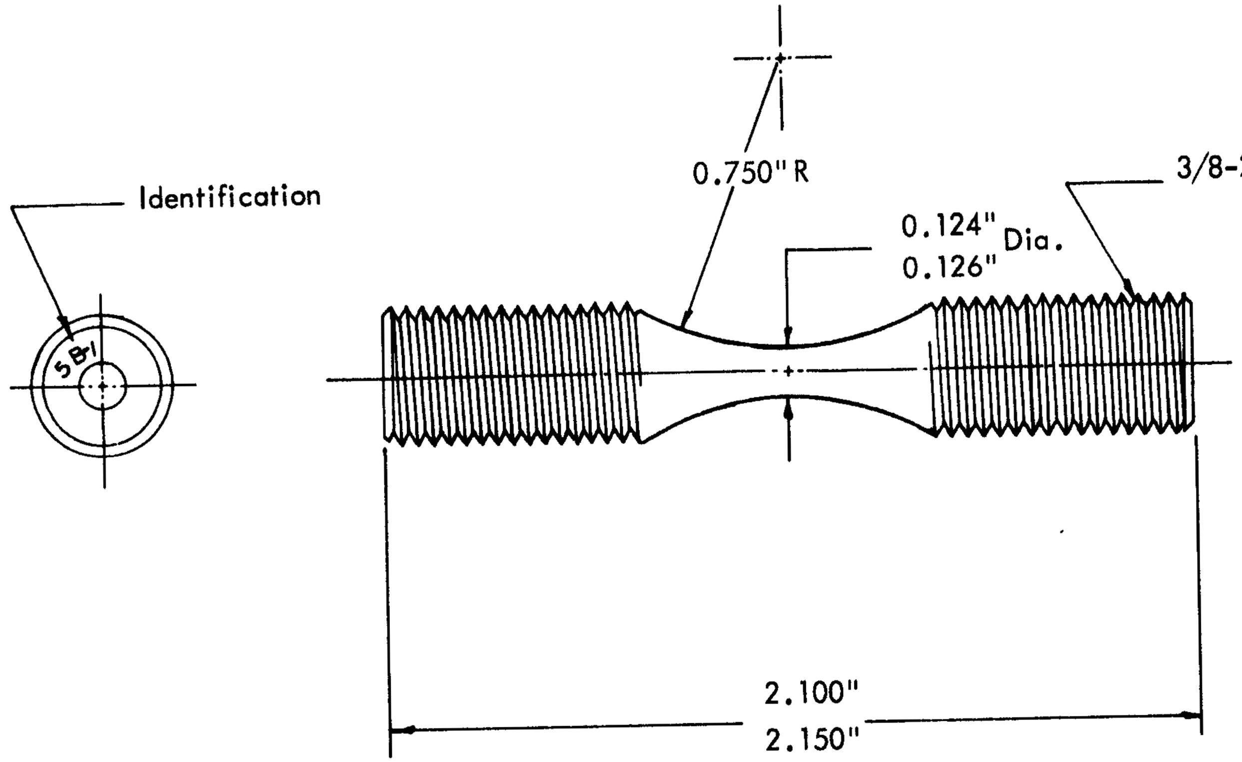

FIGURE 20 FATIGUE SPECIMEN

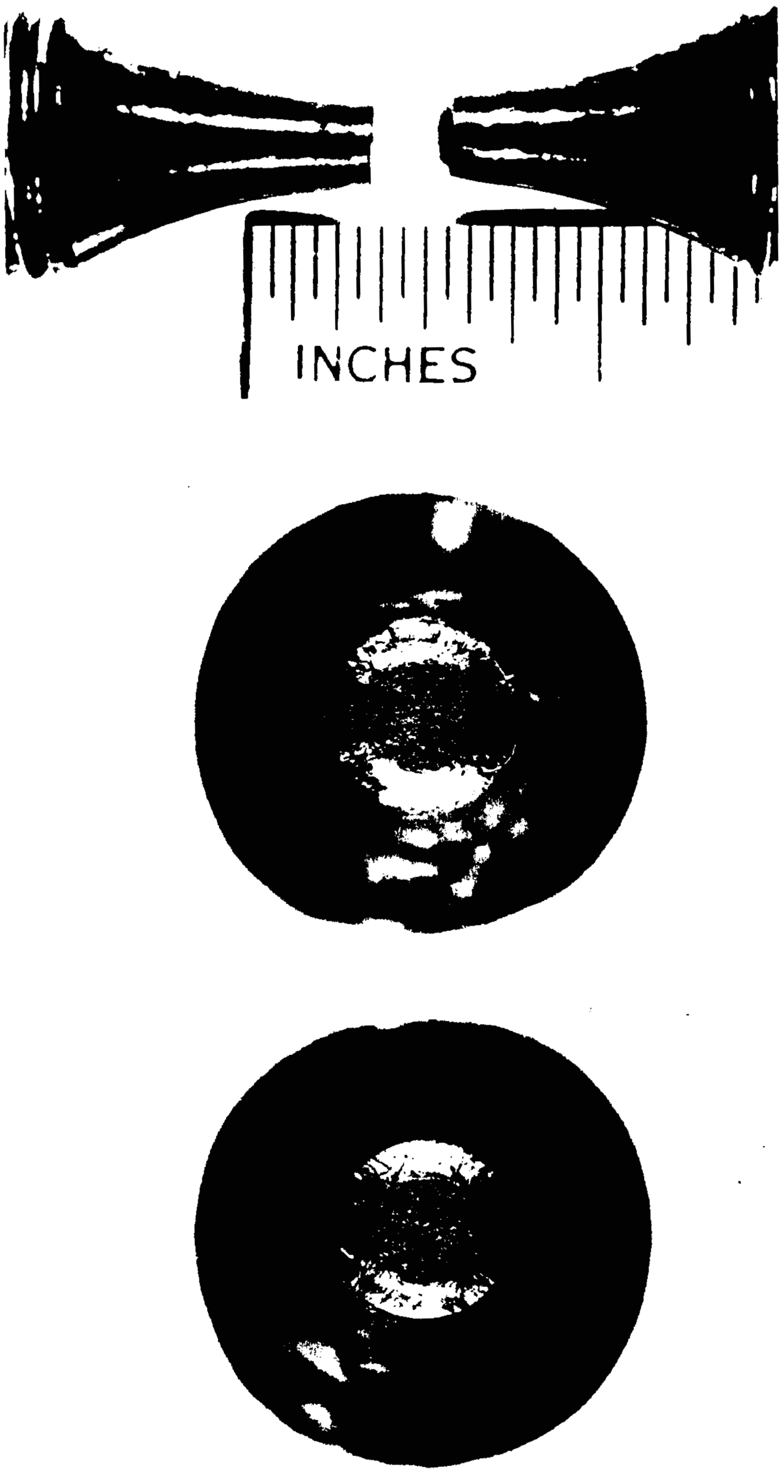

Side Elevation

View of Fracture
(cup)

View of Fracture
(cone)

FIGURE 21 FAILED 18 Ni-300 LOW-CYCLE FATIGUE SPECIMEN

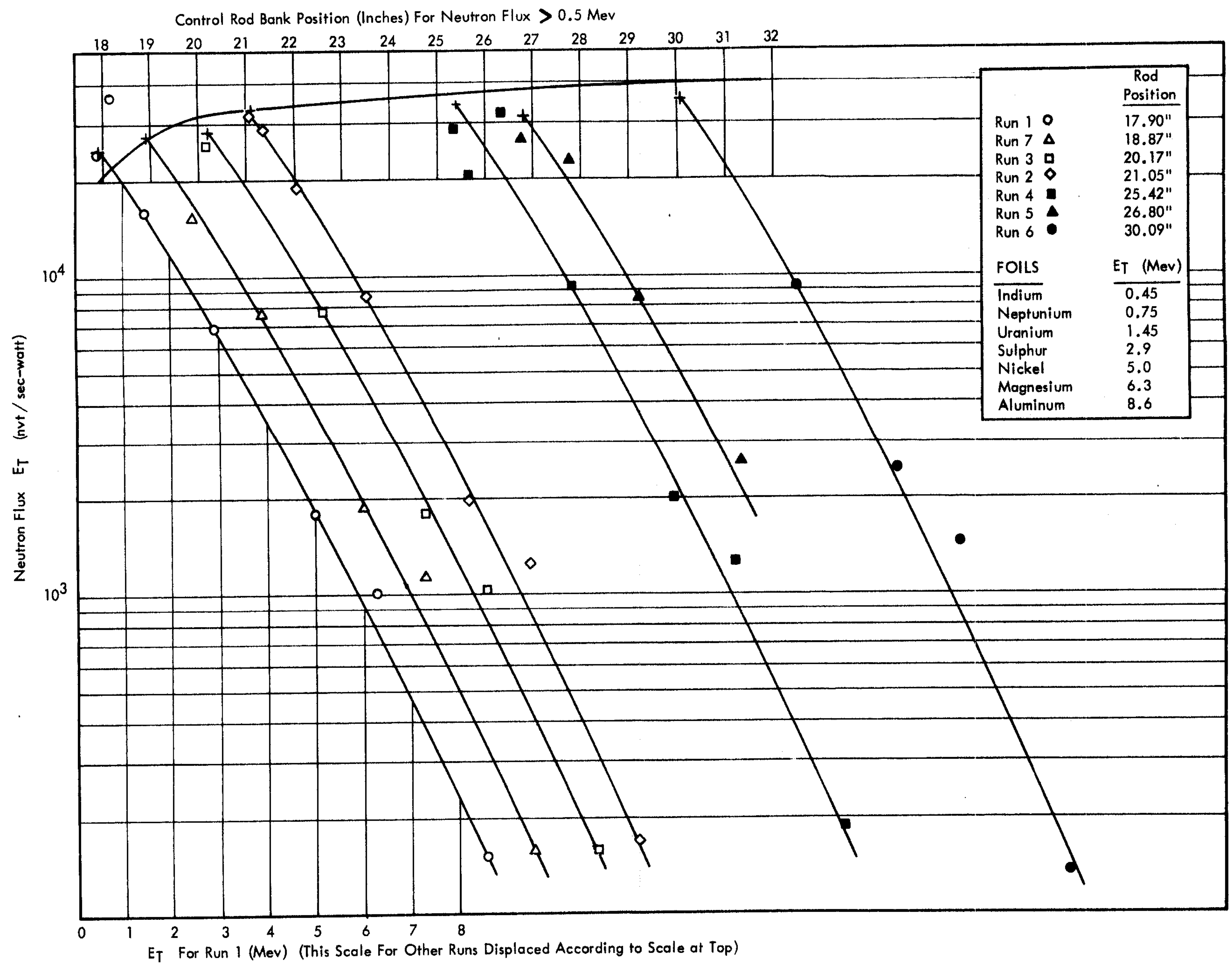

FIGURE 22 NEUTRON FLUX E_T VS. E_T AND NEUTRON FLUX 0.5 MEV VS. CONTROL ROD BANK POSITION

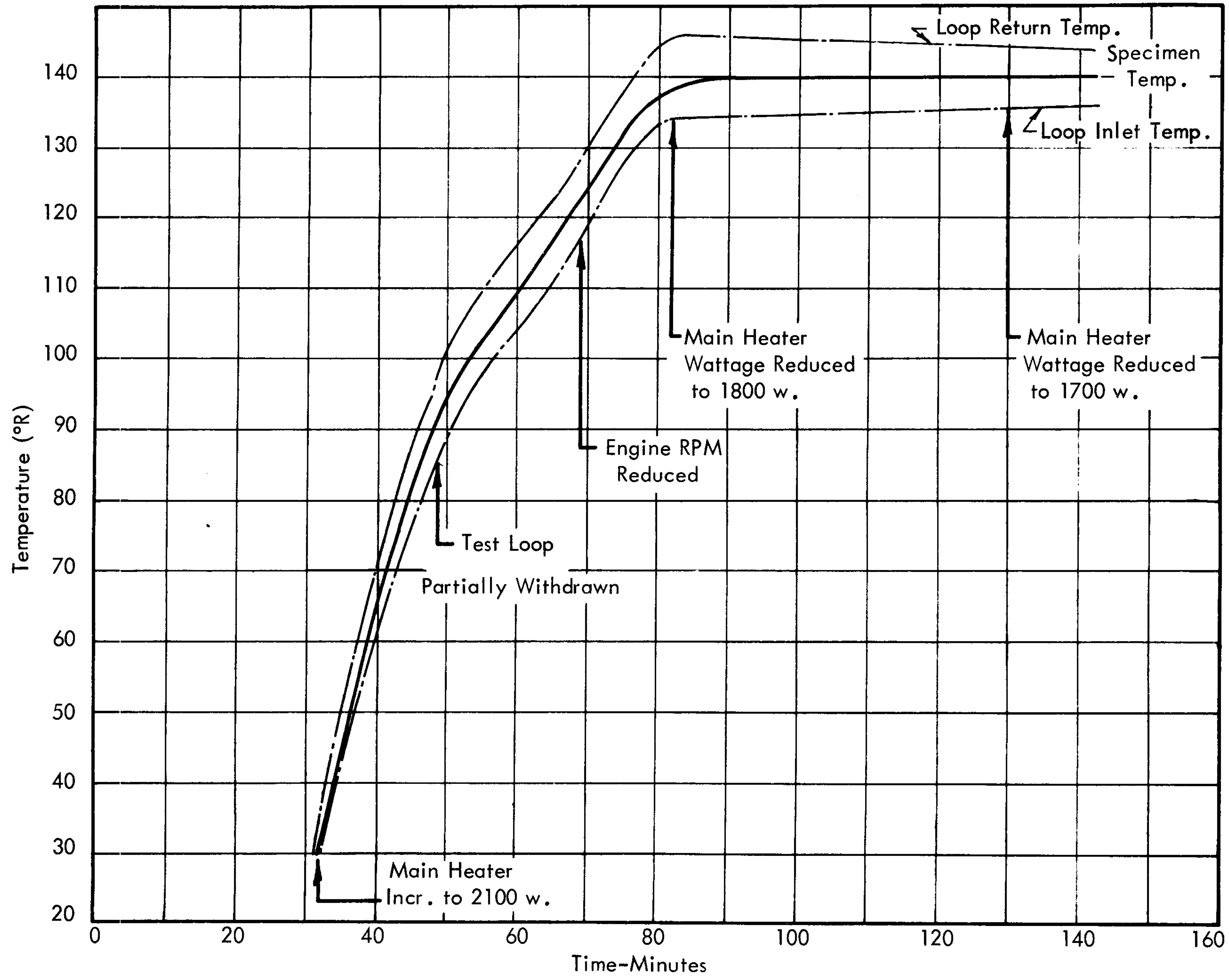

FIGURE 23 SPECIMEN WARM-UP - TYPICAL TIME-TEMPERATURE HISTORY - 30°R TO 140°R

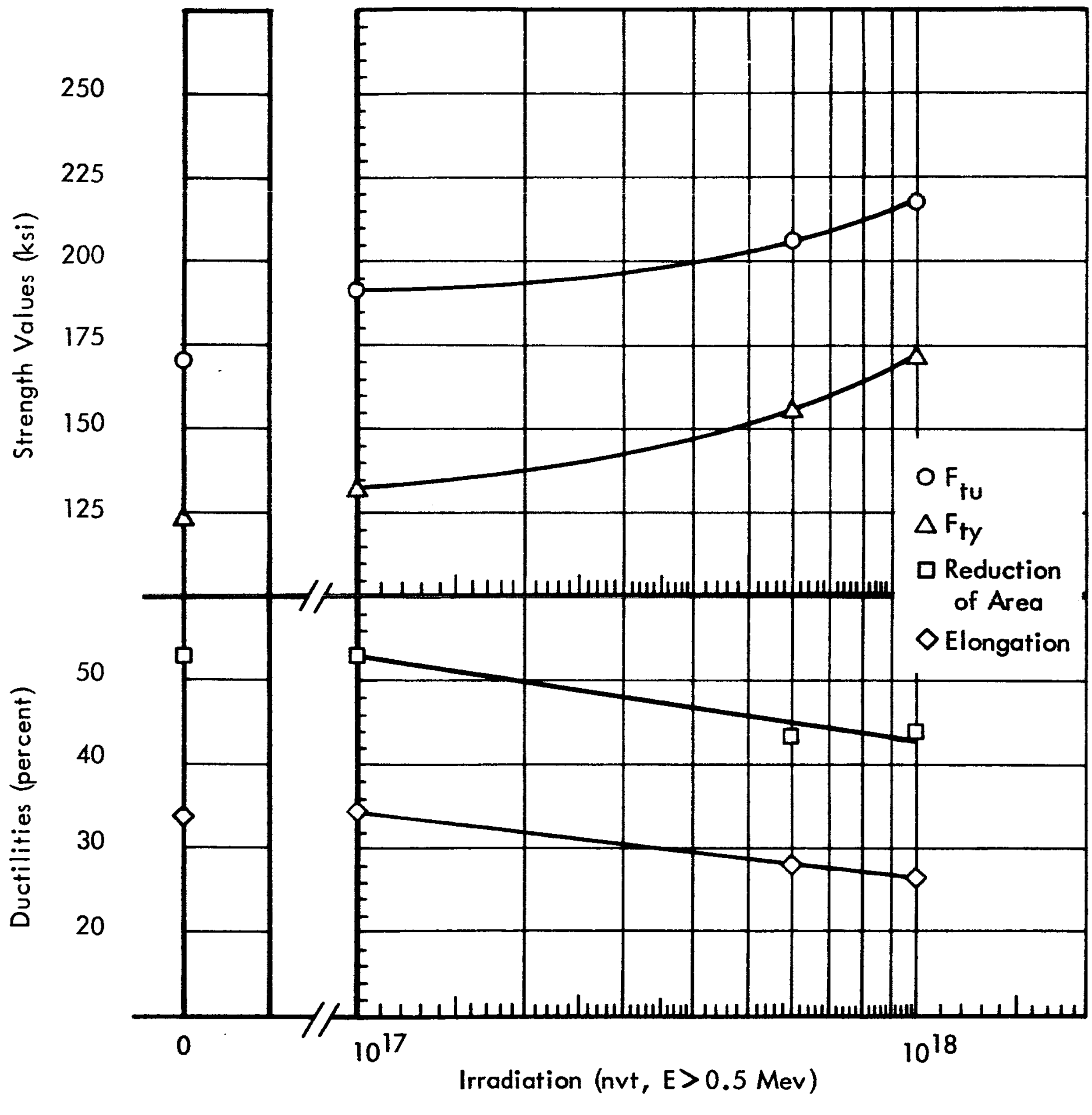

FIGURE 24 EFFECTS OF IRRADIATION AT 30°R ON TITANIUM 55A

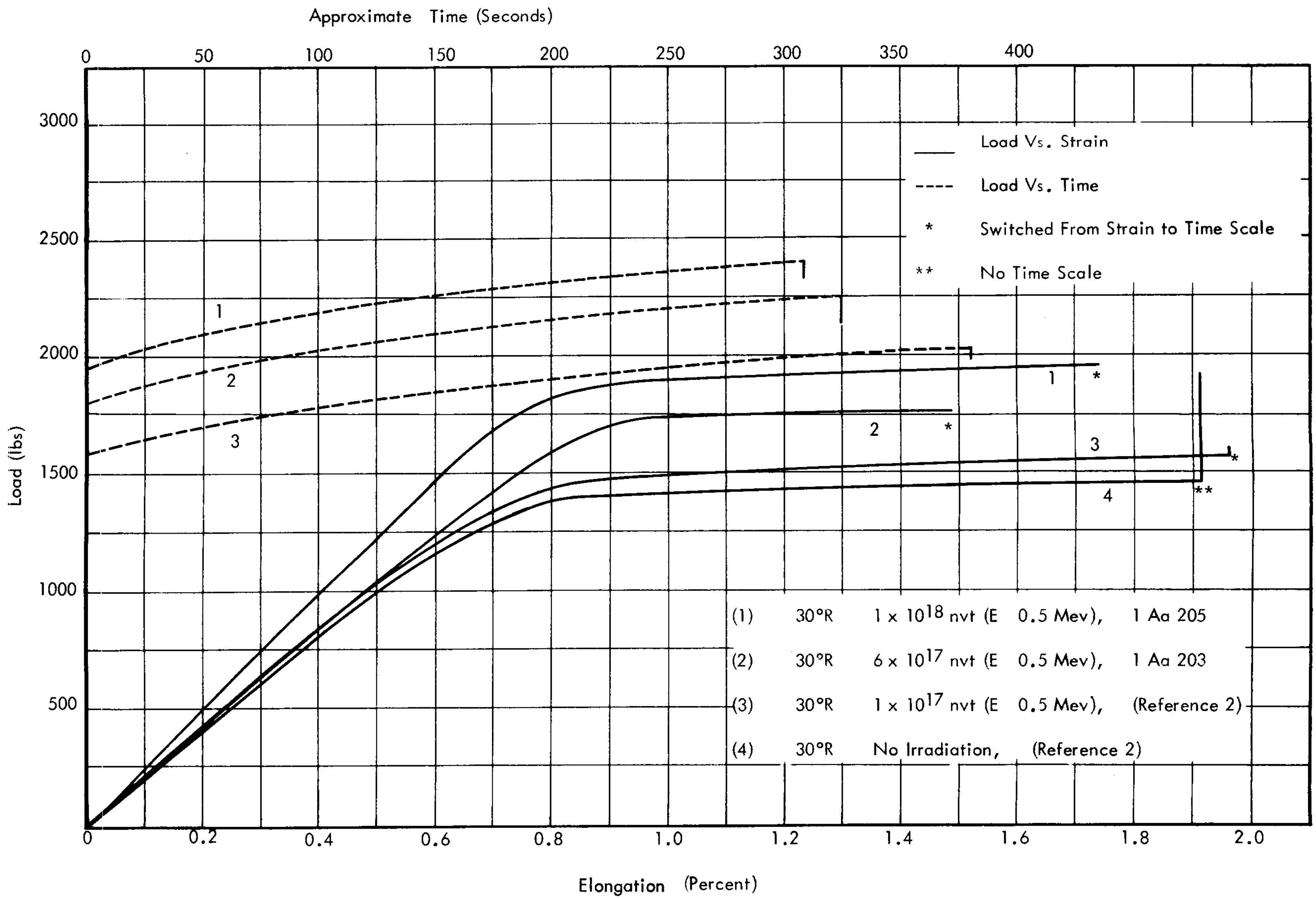

FIGURE 25 TYPICAL LOAD-ELONGATION CURVES FOR TITANIUM 55A

APPENDIX A

D I S T R I B U T I O N

NASA-Lewis Research Center (3)
21000 Brookpark Road
Cleveland, Ohio 44135
Attention: Charles L. Younger (NSD)

NASA-Lewis Research Center (1)
21000 Brookpark Road
Cleveland, Ohio 44135
Attention: T. J. Flanagan (P&SD)

NASA-Lewis Research Center (1)
21000 Brookpark Road
Cleveland, Ohio 44135
Attention: Norman T. Musial

NASA-Scientific & Technical
Information Facility (6)
Box 5700
Bethesda, Maryland 20014
Attention: NASA Representative
(CRT)

NASA-Lewis Research Center (2)
21000 Brookpark Road
Cleveland, Ohio 44135
Attention: Library

NASA-Lewis Research Center (1)
21000 Brookpark Road
Cleveland, Ohio 44135
Attention: Report Control Office

U.S. Atomic Energy Commission (3)
Technical Reports Library
Washington, D.C.

U.S. Atomic Energy Commission (1)
Division of Technical Information
Extension
P. O. Box 62
Oak Ridge, Tennessee 37831

National Aeronautics & Space
Administration (1)
Washington, D.C. 20546
Attention: George C. Deutsch
(Code RRM)

National Aeronautics & Space
Administration (1)
Washington, D.C. 20546
Attention: David Novik, Chief
(Code RNV)

AEC-NASA Space Nuclear Propulsion
Office (2)
U.S. Atomic Energy Commission
Washington, D.C. 20545
Attention: F.C. Schwenk

AEC-NASA Space Nuclear Propulsion
Office (1)
U.S. Atomic Energy Commission
Washington, D.C. 20545
Attention: J.E. Morrissey

National Aeronautics & Space
Administration (1)
Space Nuclear Propulsion Office-
Cleveland
Lewis Research Center
21000 Brookpark Road
Cleveland, Ohio 44135
Attention: L. C. Corrington

NASA-Lewis Research Center (3)
21000 Brookpark Road
Cleveland, Ohio 44135
Attention: M. H. Krasner

NASA-Lewis Research Center (1)
21000 Brookpark Road
Cleveland, Ohio 44135
Attention: H.J. Heppler, Jr.

NASA-Lewis Research Center (2)
21000 Brookpark Road
Cleveland, Ohio 44135
Attention: Dr. John C. Liwosz

NASA-Plum Brook Station (3)
Sandusky, Ohio 44870
Attention: Donald B. Crandall

NASA-Lewis Research Center (1)
21000 Brookpark Road
Cleveland, Ohio 44135
Attention: Office of Reliability & Quality Assurance

NASA-Ames Research Center (1)
Moffett Field, California 94035
Attention: Library

NASA-Flight Research Center (1)
P.O. Box 273
Edwards, California 93523
Attention: Library

NASA-Goddard Space Flight Center (1)
Greenbelt, Maryland 20771
Attention: Library

Jet Propulsion Laboratory (1)
4800 Oak Grove Drive
Pasadena, California 91103
Attention: Library

NASA-Langley Research Center (1)
Langley Station
Hampton, Virginia 23365
Attention: Library

NASA-Manned Spacecraft Center (1)
Houston, Texas 77001
Attention: Library

NASA-Western Operations (1)
150 Pico Boulevard
Santa Monica, California 90406
Attention: Library

NASA-Marshall Space Flight Center (1)
Huntsville, Alabama 35812
Attention: Library

NASA-Marshall Space Flight Center (1)
Huntsville, Alabama 35812
Attention: W.Y. Jordan, P&VE-FN

NASA-Marshall Space Flight Center (1)
Huntsville, Alabama 35812
Attention: Dr. W.R. Lucas, M-P & VE-M

NASA-Marshall Space Flight Center (1)
Huntsville, Alabama 35812
Attention: R.D. Shelton, M-RP-N

Aerojet-General Corporation (1)
P.O. Box 1947
Sacramento, California
Attention: W.A. Greenhow, Manager Radiation Effects Program Department 7431

Aerojet-General Corporation (2)
P.O. Box 1947
Sacramento, California
Attention: C.K. Soppet, Manager Nuclear Operations

Aerojet-General Corporation (3)
P.O. Box 296
Azusa, California
Attention: C.N. Trent, Associate Director
NERVA Operations

Aerojet-General Corporation (1)
P.O. Box 1947
Sacramento, California
Attention: Dr. W. Weleff

Aerojet-General Nucleonics (1)
A Division of Aerojet-General
Corporation
P.O. Box 77
San Ramon, California 94583
Attention: G. A. Linenberger,
General Manager

Aluminum Company of America (1)
P. O. Box 1012
New Kensington, Pennsylvania
Attention: Edwin H. Spuhler

Argonne National Laboratories (1)
P.O. Box 299
Lemont, Illinois
Attention: T. H. Blewitt

Argonne National Laboratory (1)
Library Services Dept. 203-CE 125
9700 South Cass Avenue
Argonne, Illinois 60440
Attention: Report Section

Arthur D. Little Company, Inc. (1)
Acorn Park
Cambridge, Massachusetts
Attention: Charles A. Schulte

Atomics International (4)
P.O. Box 309
Canoga Park, California
Attention: F. E. Farhat, Librarian

Battelle Memorial Institute (1)
505 King Avenue
Columbus, Ohio 43201
Attention: D. J. Hammon, Radiation
Effects Information Center

Battelle Memorial Institute (1)
505 King Avenue
Columbus, Ohio 43201
Attention: Roger J. Runck

Battelle-Northwest (1)
P.O. Box 999
Richland, Washington
Attention: Spencer H. Bush

Beech Aircraft Corporation (1)
P.O. Box 631
Boulder, Colorado 80301
Attention: Technical Library

The Bendix Corporation (1)
Research Laboratory Division
Southfield, Michigan
Attention: Frank W. Poblenz,
Library Services

The Boeing Company (1)
Aerospace Group
P.O. Box 3707
Seattle, Washington 98124
Attention: Ruth E. Peerenboom,
Processes Supervisor

Brookhaven National Laboratory (1)
Upton Long Island, New York 11973
Attention: D. H. Gurinsky

Brookhaven National Laboratory (1)
Upton Long Island, New York 11073
Attention: Paul W. Levy, Department
of Physics

Bureau of Naval Weapons (1)
Washington, D.C.
Attention: J.H. Terry, Captain, RRNU

California Institute of Technology (1)
1201 East California Street
Pasadena, California 91109
Attention: General Library

Carbone Company (1)
Toonton, New Jersey
Attention: E.P. Eaton

Carpenter Steel Company (1)
P.O. Box 662
Reading, Pennsylvania
Attention: Neil J. Culp

Department of the Army (1)
United States Army Munitions Command
Frankford Arsenal
Philadelphia, Pennsylvania
Attention: Librarian

Douglas Aircraft Company, Inc. (2)
Missile & Space Systems Division
3000 Ocean Park Blvd.
Santa Monica, California 90406
Attention: A2-260 Library

General Dynamics/Convair (1)
P.O. Box 1128
San Diego, California 92112
Attention: A. Hurlich, Manager
Materials & Processes Section,
Mail Zone 572-00

General Dynamics/Fort Worth (1)
P.O. Box 748
Fort Worth, Texas 76101
Attention: Mr. Bob Vollmer,
Administrative Assistant,
President's Office

General Electric Company (1)
Nuclear Materials & Propulsion
Operation
P.O. Box 132
Cincinnati, Ohio 45215
Attention: J.W. Stephenson

Hughes Aircraft Company (1)
Nucleonics Division
Fullerton, California
Attention: Dr. A.M. Liebschutz

IIT Research Institute (1)
10 W. 35th Street
Chicago 16, Illinois
Attention: D.J. McPherson,
Vice President

International Nickel Company, Inc. (1)
Huntington Alloy Products Division
Huntington, West Virginia
Attention: E.B. Fernsler

Kaman Aircraft Corporation (1)
Kaman Nuclear Division
Colorado Springs, Colorado
Attention: Mary G. Brown, Librarian

Lockheed-California Company (1)
Burbank, California 91503
Attention: Dr. Lewis Larmore,
Chief Scientist

Lockheed-California Company (2)
Burbank, California 91503
Attention: Central Library, Bldg. 63
Scientific & Technical
Information Center

Lockheed-California Company (1)
Burbank, California 91503
Attention: H.B. Wiley,
Engineering Research

Lockheed-Georgia Company (1)
Nuclear Laboratories
P.O. Box 128
Dawsonville, Georgia
Attention: Dr. M.M. Miller, Manager
Nuclear Aerospace Division

Lockheed-Georgia Company (15)
P.O. Box 2155
Sandusky, Ohio 44870
Attention: C.A. Schwanbeck

Lockheed-Georgia Company (1)
Nuclear Laboratories
P.O. Box 128
Dawsonville, Georgia
Attention: Information Center

Lockheed Missiles & Space Company (1)
3251 Hanover Street
Palo Alto, California
Attention: John C. McDonald,
Materials Research Staff

Lockheed Missiles & Space Company (2)
3251 Hanover Street
Palo Alto, California
Attention: Sci-Tech Information Center

Lockheed Missiles & Space Company (1)
3251 Hanover Street
Palo Alto, California
Attention: M.A. Steinberg, 52-30, 201

Lockheed Missiles & Space Company (1)
Sunnyvale, California
Attention: H.F. Plank, Nuclear Space
Programs

Los Alamos Scientific Laboratory (1)
P.O. Box 1663
Los Alamos, New Mexico 87544
Attention: Glen A. Graves

Los Alamos Scientific Laboratory (3)
P.O. Box 1663
Los Alamos, New Mexico 87544
Attention: Report Library

The Martin Company (1)
P.O. Box 179
Denver, Colorado 80201
Attention: F.R. Schwartzberg, G0534

Mechanical Properties Data Center (1)
Suttons Bay, Michigan 49682
Attention: Matthew J. Kanold,
Administrative Assistant

National Bureau of Standards (1)
Boulder, Colorado 80302
Attention: Cryogenic Data Center

National Bureau of Standards (1)
Cryogenic Engineering Laboratory
Boulder, Colorado 80302
Attention: R.P. Reed

North American Aviation (1)
Rocketdyne Division
6633 Canoga Avenue
Canoga Park, California
Attention: Technical Information
Center

Northrop Corporation (1)
Norair Division
3901 W. Broadway
Hawthorne, California
Attention: Technical Information
3343-32

Oak Ridge National Laboratory (1)
Oak Ridge, Tennessee 37831
Attention: D.S. Billington

Ohio State University Libraries (1)
Serial Division
1858 Neil Avenue
Columbus, Ohio 43210

Pennsylvania State University (1)
105 Hammond Building
University Park, Pennsylvania 16802
Attention: Mr. Joseph Marin, Engineering
Mechanics Department

Picatinny Arsenal (1)
Technical Information Section,
SMUPA-VA6
Dover, New Jersey 07801
Attention: Commanding Officer

Purdue University (1)
Lafayette, Indiana
Attention: Librarian

Pure Carbon Company (1)
Wellsville Street
Saint Marys, Pennsylvania
Attention: Robert Paxon

Reynolds Metals Company (1)
6601 West Broad Street
Richmond, Virginia
Attention: L.E. Householder

Rice University (1)
P.O. Box 1892
Houston, Texas 77001
Attention: The Fondren Library

Rocketdyne (1)
A Division of North American
Aviation, Inc.
6633 Canoga Avenue
Canoga Park, California
Attention: Mr. G. A. Fairboirn,
D/596-174Z-2

Sandia Corporation (1)
P.O. Box 5800
Sandia Base
Albuquerque, New Mexico 87115
Attention: Technical Library

Southeastern Research Institute (1)
Birmingham, Alabama
Attention: J. R. Kattus

Special Metals, Inc. (1)
New Hartford, New York
Attention: Robert Neilsen

Titanium Metals Corporation of America (1)
233 Broadway
New York, New York
Attention: E.F. Erbin, Staff

TRW Systems (1)
Technical Information Center
One Space Park
Redondo Beach, California 90278

U.S. Air Force (1)
Air Force Weapons Laboratory
Kirtland AFB, New Mexico 87117
Attention: Technical Library (WLIL)

U.S. Air Force (1)
AF Materials Laboratory, Research & Technology Division, AFSC
Wright-Patterson AFB, Ohio 45433
Attention: Harold M. Hormann

U.S. Air Force (1)
Foreign Technology Division, TDEPR
Wright-Patterson AFB, Ohio 45433
Attention: Lt. Schauffle

U.S. Air Force (1)
AFML (MAAM) (1A)
Wright-Patterson AFB, Ohio 45433

U.S. Army Materials Research Agency (1)
Watertown Arsenal
Watertown, Massachusetts
Attention: T.S. DeSisto

U.S. Naval Research Laboratory (1)
Washington, D.C. 20390
Attention: Dr. Albert V.H. Masket, Mechanics Division, Code 6204

U.S. Naval Research Laboratory (1)
Washington, D.C. 20390
Attention: L.E. Steele, Head, Reactor Materials Branch, Metallurgy Division

United States Steel Corporation (1)
Monroeville, Pennsylvania
Attention: Waldo Rall

University of California (1)
Lawrence Radiation Laboratory
Berkeley, California
Attention: Technical Information Division

University of California (1)
Lawrence Radiation Laboratory
P.O. Box 808
Livermore, California
Attention: Technical Information Division

University of California (1)
Los Alamos Scientific Laboratory
P. O. Box 1663
Los Alamos, New Mexico 87544
Attention: W.L. Kirk

University of California (1)
405 Hilgard Avenue
Los Angeles, California 90024
Attention: Engineering & Mathematical Sciences Library

University of California (1)
University Research Library
Los Angeles, California 90024
Attention: Serials Department

University of Chicago (1)
5640 Ellis
Chicago, Illinois 60637
Attention: Institute of Metals Library

University of Colorado (1)
Engineering Research Center
Boulder, Colorado
Attention: K.D. Timmerhaus, Associate Dean of Engineering

University of Georgia Libraries (2)
Athens, Georgia 30601
Attention: Acquisitions Division

University of Michigan (1)
Ann Arbor, Michigan 48104
Attention: Robert G. Carter, University Library

Westinghouse Electric Corporation (1)
Astronuclear Laboratory
P.O. Box 10864
Pittsburgh, Pennsylvania 15235
Attention: Dr. D.E. Thomas, Manager
Materials Department

Westinghouse Electric Corporation (1)
Metallurgical Division
Pittsburgh, Pennsylvania 15235
Attention: E.T. Wessel, Research &
Development Center

ABSTRACT

This is the second quarterly report for a study of the effects of nuclear radiation on materials at cryogenic temperatures. These studies include the effect of: (1) 10^{18} nvt at 30°R on tensile properties of titanium base alloys; (2) irradiation temperature (30°R to 540°R) on tensile properties of Aluminum 1099 - H14 following irradiations up to 3×10^{17} nvt; (3) annealing following irradiation at 30°R to 10^{17} nvt on tensile properties of Aluminum 1099; and (4) irradiation at 30°R on axial, low-cycle fatigue properties of titanium base alloys. This report describes maintenance of and modifications to existing test equipment, required neutron flux mapping and tensile test results from Titanium 55A and partial tensile test results from Aluminum 1099.

ABSTRACT

This is the second quarterly report for a study of the effects of nuclear radiation on materials at cryogenic temperatures. These studies include the effect of: (1) 10^{18} nvt at 30°R on tensile properties of titanium base alloys; (2) irradiation temperature (30°R to 540°R) on tensile properties of Aluminum 1099 - H14 following irradiations up to 3×10^{17} nvt; (3) annealing following irradiation at 30°R to 10^{17} nvt on tensile properties of Aluminum 1099; and (4) irradiation at 30°R on axial, low-cycle fatigue properties of titanium base alloys. This report describes maintenance of and modifications to existing test equipment, required neutron flux mapping and tensile test results from Titanium 55A and partial tensile test results from Aluminum 1099.